Cardiac noradrenergic deficiency revealed by [18]F-dopamine positron emission tomography identifies preclinical central Lewy body diseases

David S. Goldstein,[1] Courtney Holmes,[1] Patti Sullivan,[1] Grisel Lopez,[2] Janna Gelsomino,[1] Sarah Moore,[1] Risa Isonaka,[1] Tianxia Wu,[3] Yehonatan Sharabi[4]

[1]*Autonomic Medicine Section, Clinical Neurosciences Program, Division of Intramural Research, National Institute of Neurological Disorders and Stroke, National Institutes of Health, Bethesda, MD 20892;* [2]*Molecular Neurogenetics Section, National Human Genome Research Institute, National Institutes of Health, Bethesda, MD 20892;* [3]*Clinical Trials Unit, Office of the Clinical Director, Division of Intramural Research, National Institute of Neurological Disorders and Stroke, National Institutes of Health, Bethesda, MD 20892;* [4]*Chaim Sheba Medical Center, Tel-Aviv University, Tel-Hashomer, Israel*

Corresponding author: David S. Goldstein, MD PhD, Autonomic Medicine Section, NINDS, NIH, 10 Center Drive MSC-1620, Building 10 Room 8N260, Bethesda, MD 20892-1620 USA. iPhone: 301-675-1110, e-mail: goldsteind@ninds.nih.gov. ORCID: 0000-0002-5709-9940

Short title: [18]F-DA PET Predicts Central LBDs

Manuscript counts: Title words: 15; Abstract words: 250; Figures: 11; Tables: 4; References: 89. Supplementary Tables: 2. Supplementary Figures: 1

Keywords: Lewy; Parkinson; fluorodopamine; sympathetic; norepinephrine

Conflict of interest: The authors have declared that no conflict of interest exists.

ABSTRACT

Background: In the Lewy body diseases (LBDs) Parkinson's disease (PD) and dementia with Lewy bodies (DLB), by the time parkinsonism or cognitive dysfunction manifests clinically substantial neurodegeneration has already occurred. Biomarkers are needed to identify central LBDs in a preclinical phase, when neurorescue strategies might forestall symptomatic disease. This phase may involve catecholamine deficiency in the autonomic nervous system. We analyzed data from the prospective, observational, long-term PDRisk study to assess the predictive value of low vs. normal cardiac ^{18}F-dopamine positron emission tomography (PET), an index of myocardial content of the sympathetic neurotransmitter norepinephrine, in at-risk individuals.

Methods: Participants self-reported risk factor information (genetics, olfactory dysfunction, dream enactment behavior, orthostatic intolerance or hypotension) at a protocol-specific website. Thirty-four with ≥3 confirmed risk factors underwent serial cardiac ^{18}F-dopamine PET at 1.5-yearly intervals for up to 7.5 years or until PD was diagnosed.

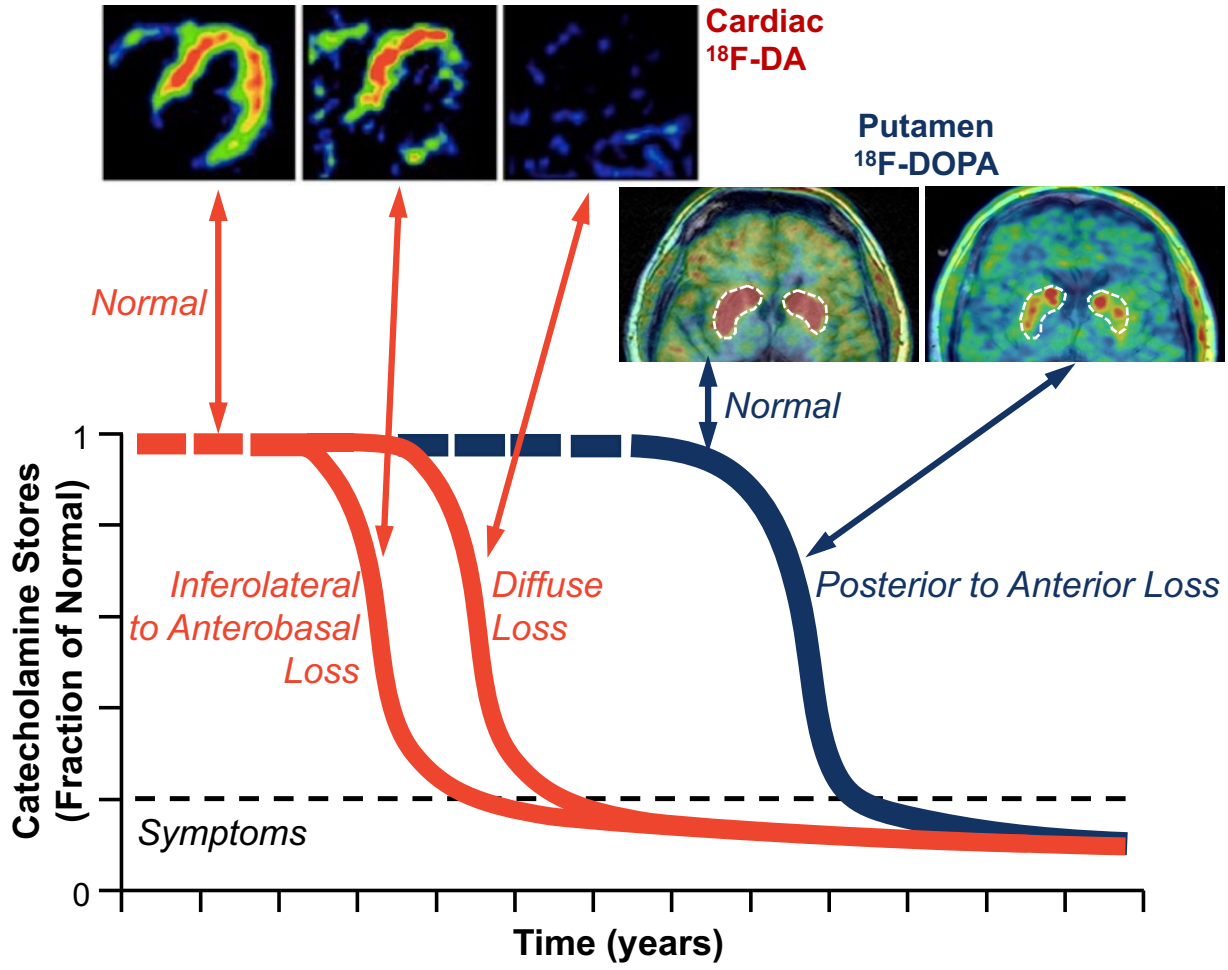
Results: Upon initial evaluation, 9 participants had low myocardial ^{18}F-dopamine-derived radioactivity (<6,000 nCi-kg/cc-mCi) and 25 normal radioactivity. During follow-up, 8 of the 9 with low initial radioactivity were diagnosed with a central LBD (LBD+), in contrast with 1 of 25 with normal radioactivity (log-rank test p=0.0091). Conversely, all of 9 LBD+ participants had low ^{18}F-dopamine-derived radioactivity before or at the time of diagnosis of a central LBD, whereas among 25 participants without a central LBD only 1 (4%) had persistently low radioactivity (p<0.0001 by Fisher's exact test).

Conclusion: Cardiac ^{18}F-dopamine PET highly efficiently distinguishes at-risk individuals who are diagnosed subsequently with a central LBD from those who are not.

Trial registration: ClinicalTrials.gov NCT00775853

Funding: Division of Intramural Research, NIH, NINDS

GRAPHICAL ABSTRACT



INTRODUCTION

Aging-related neurodegenerative diseases are posing an increasing public health burden worldwide as populations are getting older. Prominent among these conditions are the central Lewy body diseases (LBDs) Parkinson's disease (PD) and dementia with Lewy bodies (DLB).

By the time a person develops symptoms or signs of a central LBD, it is likely that substantial central neurodegeneration has already occurred. There is an urgent need for biomarkers that can detect the pathophysiological process in a preclinical phase, when strategies such as lifestyle modifications, dietary supplements, or prophylactic medications might delay the onset of or even prevent symptomatic disease.

PD and DLB entail cardiac sympathetic denervation, as documented by in vivo neuroimaging (1, 2) and post-mortem histopathology (3) and neurochemistry (4). Indeed, in PD there is as much depletion of the sympathetic neurotransmitter norepinephrine in the left ventricular myocardium (5) as there is of the closely related catecholamine dopamine in the putamen (6), the main site of catecholamine deficiency in the brain. DLB involves at least as frequent cardiac noradrenergic deficiency as does PD (7, 8). Except in isolated cases (9, 10), however, whether cardiac noradrenergic deficiency precedes central LBDs has been unknown. Thus, although it is widely suspected that the pathogenetic process leading to PD can begin outside the brain, with early involvement of the autonomic nervous system (11-14), to date this key issue has not been addressed directly in a prospective, long-term follow-up study.

The recently completed intramural NINDS PDRisk study (NCT00775853) was designed to determine whether in people with multiple PD risk factors, biomarkers of catecholamine deficiency in the heart or brain predict PD during long-term follow-up. Entry into the PDRisk study was based on four categories of risk—genetic, olfactory, dream enactment behavior (as in rapid eye movement behavior disorder (RBD)), and orthostatic intolerance or orthostatic hypotension (OH), all of which have been reported to precede the onset of both PD (15-18) and DLB (19-23).

A "first look" at the data (24) revealed that in at-risk individuals, a validated biomarker of

depleted myocardial norepinephrine stores, low myocardial concentrations of the sympathetic neuroimaging agent ^{18}F-dopamine quantified by positron emission tomography (PET) (25) predicted PD at 3 years of follow-up. The data obtained at this early point in the study did not address the meaning of persistently negative biomarkers or conversion from negative to positive biomarkers during follow-up; the possible spatio-temporal sequence from an early cardiac sympathetic to a later nigrostriatal dopaminergic lesion; or mechanisms of cardiac noradrenergic deficiency, which as explained below are relevant to potential experimental neuroprotective trials. The results of the initial report justified continuation and expansion of the study, with more participants followed for longer time periods (up to 7.5 years with approximately 1.5-yearly inpatient evaluations), in order to assess the relative risks associated with low vs. normal ^{18}F-dopamine-derived radioactivity. Accrual into the PDRisk study and follow-up testing have been completed as called for by the power calculation when the study was designed (see Methods). Since the same risk factors apply for DLB, the analysis was extended to DLB as an outcome measure.

In addition to ^{18}F-dopamine PET, participants underwent brain ^{18}F-DOPA PET to assess the integrity of putamen dopaminergic terminals (26, 27), with magnetic resonance imaging for anatomic registration of ^{18}F-DOPA PET scans in the same subjects using the PMOD image analysis package (28). Other tests included ^{13}N-ammonia PET to adjust ^{18}F-dopamine-derived radioactivity for myocardial perfusion (29); lumbar puncture for assaying cerebrospinal fluid (CSF) levels of catechols such as 3,4-dihydroxyphenylacetic acid (DOPAC), the main neuronal metabolite of dopamine (30); and physiological and neurochemical autonomic function testing (31-33). The serial nature of the PET imaging enabled examination of whether cardiac noradrenergic abnormalities precede nigrostriatal dopaminergic abnormalities, as one would expect if central LBDs entailed early involvement of the sympathetic innervation of the heart (12, 13).

To examine mechanisms of cardiac noradrenergic deficiency, we applied indices of denervation and of dysfunction in residual nerves (“sick-but-not-dead” phenomenon (34)).

Distinguishing between the two determinants of cardiac noradrenergic deficiency is relevant to potential experimental therapeutic trials, because, put bluntly, you can't treat neurons that are dead, whereas neurons that are dysfunctional but alive (5) might be rescued (35).

We paid particular attention to the possibility of decreased efficiency of vesicular sequestration of cytoplasmic catecholamines via the type 2 vesicular monoamine transporter (VMAT2). A vesicular storage defect would not only deplete releasable neurotransmitter stores but also promote autotoxicity from augmented oxidation of cytoplasmic catecholamines (36-38). Diminished vesicular storage in existing nerve terminals could have any of several causes, such as decreased mitochondrial complex 1 activity (39), alpha-synuclein (αS) oligomers (36, 40), or decreased VMAT2 availability (41), all of which are potential therapeutic targets; however, no previous study has determined whether indices of attenuated vesicular sequestration in cardiac sympathetic nerves precede central LBDs in at-risk individuals.

One way to examine separately denervation vs. decreased vesicular storage is pharmacokinetic, by tracking the rapid early rise in ^{18}F-dopamine-derived radioactivity and the relatively slow subsequent fall from the peak value across dynamic PET frames (42). Denervation would be expected to decrease the rate of accumulation of ^{18}F-dopamine-derived radioactivity in the myocardium, because tissue uptake of the tracer depends on the cell membrane norepinephrine transporter, which is missing in the setting of sympathetic denervation (43). The loss of cardiac sympathetic nerves would shift downward the curve relating ^{18}F-dopamine-derived radioactivity to time across all the dynamic frames in a PET session, without affecting the rate of decline in radioactivity from the peak value. In contrast, if there were decreased vesicular storage, then after the peak in ^{18}F-dopamine-derived radioactivity the subsequent "washout" of radioactivity would be accelerated (42).

In summary, in this prospective, observational, long-term follow-up study we asked whether among individuals with multiple PD risk factors cardiac sympathetic denervation or dysfunction revealed by ^{18}F-dopamine PET separates the group subsequently diagnosed with a central LBD (LBD+) from the group not so diagnosed (LBD-). The study also addressed whether

the results of serial ^{18}F-dopamine and ^{18}F-DOPA PET support a sequence of pathophysiologic progression from cardiac noradrenergic to putamen dopaminergic deficiency.

RESULTS

Subject Accrual

Data collection in the PDRisk study began in 2009 and ended in January 2023, after the last follow-up visit of the last participant. A total of 2,094 individuals registered for the study and provided their risk factor information at the protocol-specific website (Figure 1). Of these, 339 (16%) reported ≥3 risk factors and were considered eligible for further participation. After phone interviews of eligible candidates by a Research Nurse, 82 at-risk individuals came to the National Institutes of Health (NIH) Clinical Center for on-site screening, gave written informed consent, and were considered accrued (PDRisk cohort). One at-risk subject was withdrawn during the first admission because of a previously undisclosed exclusion criterion.

Subject Groups

Thirty-four of the accrued subjects in the PDRisk study had confirmation of ≥3 risk factors (PDRisk+) at the time of on-site screening, while 48 accrued subjects did not (PDRisk-) and were not followed as inpatients (Figure 1, Supplemental Table 1).

Included in the PDRisk+ group were 2 individuals who had been tested under another protocol and satisfied the eligibility criteria and consented to follow-up under the PDRisk protocol. For the purposes of data analysis, the follow-up period for these participants began with their first evaluation at the NIH.

Of the 34 accrued subjects with ≥3 confirmed risk factors, 9 (26%) subsequently developed a central LBD (LBD+ group; 6 with PD, 2 DLB, and 1 PD+dementia). One participant was diagnosed with PD by the blinded neurologist; however, the patient's death certificate showed she had died of multiple system atrophy (MSA), which is not a LBD, and she was assigned to the LBD- group (LBD- #20). This case is described later in detail.

The LBD+ and LBD- groups had similar mean total numbers of risk factors and did not differ in the numbers with a positive family history of PD, olfactory dysfunction, dream enactment behavior, or symptoms of orthostatic intolerance (Supplementary Table 1). The LBD+ and LBD- groups also did not differ in sex or age at study entry or in prescribed medications

(Supplementary Table 1). Median follow-up was 2.8 years in the LBD+ group and 6.3 years in the LBD- group.

Data from 11 concurrently studied Healthy Volunteers (HV) were included. Of the 11 HVs, 8 had neuroimaging data. Seven HVs were accrued under the PDRisk protocol and the remainder under other IRB-approved protocols.

Incidence of diagnosed central LBDs in groups stratified by initial [18]F-dopamine-derived radioactivity

Nine PDRisk study participants had low initial myocardial [18]F-dopamine-derived radioactivity (<6,000 nCi-kg/cc-mCi). Of the 9, 8 (89%) were diagnosed subsequently with a central LBD (LBD+), in contrast with 1 of 25 (4%) participants with normal initial radioactivity ($p<0.0001$ by Fisher's exact test). In the group with low initial radioactivity the median duration of follow-up was 8.1 years, and in the group with normal initial radioactivity the median duration of follow-up was 6.1 years.

Kaplan-Meier curves generated for the dichotomized initial [18]F-dopamine-derived radioactivity in the 8' dynamic PET frame showed that throughout the period of follow-up the fraction of subjects with low radioactivity who developed a central LBD was greater than that of subjects with normal radioactivity (log-rank $p=0.0091$; Figure 2).

Initial cardiac [18]F-dopamine-derived radioactivity in the LBD+ vs. LBD- groups

Nine participants were diagnosed with a central LBD during follow-up (LBD+ group). Of these, 8 (89%) had low initial [18]F-dopamine-derived radioactivity. There were 25 participants who were not diagnosed with a central LBD (LBD- group); of these, 1 (4%) had low initial radioactivity ($p<0.0001$ by Fisher's exact test; Figure 3).

Analyses of variance with Tukey's post-hoc test showed that for 6 biomarkers of [18]F-dopamine-derived radioactivity the differences between the LBD+ and the LBD- and HV groups were significant, whereas the HV and LBD- groups did not differ (Table 1). In this analysis, age was used as a covariate, while sex was not associated with any outcomes and was dropped as a covariate.

Receiver operating characteristic (ROC) curves were constructed to evaluate the measures of ^{18}F-dopamine-derived radioactivity in terms of their efficiency in separating the LBD+ from the LBD- groups (Figure 4, Table 2). Based on the areas under the ROC curves (AUCs), all of 6 biomarkers showed a high degree of separability (AUC ≥ 0.85). Sensitivities and specificities based on Youden's method, tabulated in Table 2, showed high values for the 6 biomarkers, comparing the LBD+ group vs. the LBD- subgroup with ≥7 years of follow-up and vs. the entire LBD- group.

Trends in cardiac ^{18}F-dopamine-derived radioactivity during follow-up in the LBD+ and LBD- groups

The linear random coefficient model analysis showed that in both the LBD+ and LBD- groups cardiac ^{18}F-dopamine-derived radioactivity was stable over years of follow-up (Figure 5).

Comparisons of kinetics of ^{18}F-dopamine-derived radioactivity within PET sessions in LBD+, LBD-, and HV groups

In all subjects cardiac ^{18}F-dopamine-derived radioactivity increased rapidly during the 3-minute administration of the tracer (Figure 6; Table 3). In general, the LBD+ and LBD- groups differed in septal ^{18}F-dopamine-derived radioactivity at all time points after the 3-minute administration of the tracer, whereas the LBD- and HV groups did not differ at any time point.

The mono-exponential slope of decline in radioactivity between the peak value and 25', $k_{Max\text{-}25'}$, was greater in the LBD+ than the LBD- group ($p<0.001$; Figure 3B). Conversely, of 9 subjects with $k_{Max\text{-}25'} \geq 0.028$ min^{-1} when they were first evaluated, 8 (89%) subsequently were diagnosed with a central LBD, in contrast with 1 of 25 (4%) subjects with $k_{Max\text{-}25'} < 0.028$ min^{-1} ($p<0.0001$ by Fisher's exact test; Table 2).

Because of the observed non-linear changes in ^{18}F-dopamine-derived radioactivity over time within PET sessions, a piecewise linear random coefficient model analysis with a single breakpoint was performed from time=1' to peak time (with breakpoint at time=3') and separately from time=peak time to 25' (breakpoint at time=13').

Table 3 and Figure 7 show the results of the random coefficient model analysis with breakpoint at time = 3' for the early increase from time = 1' to the time of peak ^{18}F-dopamine-derived radioactivity. As expected, in each of the LBD+, LBD-, and HV groups the slope for time ≤ 3' was significantly different from 0. The slope for time = 3' to maximum radioactivity was not significant for the LBD+ group but was significant for the other two groups. For each group, the difference in slope between time ≤ 3' and time ≥ 3' was significant, and the increase (slope > 0 nCi-kg/cc-mCi per minute) for time ≤ 3' was faster than after time ≥ 3'. For time ≤ 3' the difference in slope between the LBD+ and the HV and LBD- groups was significant, whereas the difference in slope between the HV and LBD- groups was not significant.

In summary, the random coefficient model analysis for time = 1' to the time of peak radioactivity revealed decreased uptake of ^{18}F-dopamine in the LBD+ group during the 3-minute infusion of the tracer.

For assessing the decline in ^{18}F-dopamine-derived radioactivity from the peak value, the radioactivity data were standardized by the maximum radioactivity across all the frames in the PET session. In the period from peak time to 13', the decline (negative slope) in radioactivity was significantly faster in the LBD+ group than in the HV and LBD- groups ($p<0.001$, Table 3; Figure 7B, 7D); the slopes did not differ between the HV and LBD- groups ($p=0.1925$). In contrast, in the period of time=13' to 25', the slope of decline in radioactivity in the LBD+ group was significantly slower than in the HV and LBD- groups ($p<0.0001$), and the slopes did not differ between the HV and LBD- groups ($p=0.4188$).

In summary, the random coefficient model analyses for time=peak time to 25' showed more rapid proportionate loss of ^{18}F-dopamine-derived radioactivity in the LBD+ group between the peak radioactivity and 13' but not between 13' and 25'.

Correlations among biomarkers of cardiac noradrenergic deficiency

The 6 biomarkers of ^{18}F-dopamine-derived radioactivity were significantly correlated, based on both Pearson and Spearman correlation coefficients (Supplementary Table 2). The correlation coefficients between $k_{Max\text{-}25}$, and the other 5 biomarkers were moderately negatively

correlated, with the extent of correlation related to the time of the dynamic frame (relatively high Pearson r values for the 8', 13', 18', and 25' frames (r=-0.63, -0.56, -0.67, -0.70, p<0.0001 each)).

Biomarkers of central dopaminergic innervation and relationships to biomarkers of cardiac noradrenergic innervation

The LBD+ group had lower mean initial CSF levels of DOPAC, lower putamen/occipital cortex (PUT/OCC) ratios of ^{18}F-DOPA-derived radioactivity, and greater putamen washout percents of ^{18}F-DOPA-derived radioactivity than did the LBD- group (Figure 3D-F).

Among the LBD+ participants, in 4 the PUT/OCC ratio of ^{18}F-DOPA-derived radioactivity initially was above the cutoff value (2.7) (Figure 8). All 4 had a decrease in their PUT/OCC ratios between the initial evaluation and the time of diagnosis of a central LBD. Moreover, in 3 of the 4, by the time they reached the study endpoint their PUT/OCC ratios were below the cutoff value. Four individuals in the LBD+ group had initial washout percents of putamen ^{18}F-DOPA-derived radioactivity that were below the cutoff value (20%). All 4 had increases in their washout percents between the time of initial evaluation and the time of diagnosis of a central LBD; in 3 of the 4, by the time they reached the study endpoint their washout percents were above the cutoff value. In summary, in a substantial minority of the LBD+ group low cardiac ^{18}F-dopamine-derived radioactivity preceded low putamen ^{18}F-DOPA-derived radioactivity.

Across the LBD+, LBD-, and HV groups, individual values for washout percents of putamen ^{18}F-DOPA-derived radioactivity were negatively correlated with PUT/OCC ratios and CSF DOPAC levels, while PUT/OCC ratios were unrelated to CSF DOPAC levels (Supplementary Table 2). Individual values for the washout percents of putamen ^{18}F-DOPA-derived radioactivity were strongly negatively correlated with cardiac ^{18}F-dopamine-derived radioactivity in the PET frames from 8' to 25' (Supplementary Table 2). Washout percents of putamen ^{18}F-DOPA-derived radioactivity were unrelated to values for cardiac $k_{Max\text{-}25'}$.

Myocardial perfusion

Myocardial perfusion as indicated by interventricular septal myocardial [13]N-ammonia derived radioactivity did not distinguish the LBD+ from the LBD- and HV groups (Figure 3C).

Autonomic function tests

Supplementary Table 1 (Physiological Initial tab) summarizes the data from autonomic function testing upon initial evaluation in the LBD+ and LBD- groups. Data from the LBD- patient with MSA were excluded from the statistical analyses. The LBD+ group had lower mean heart rates during supine rest ($p=0.00439$) and head-up tilt ($p=0.02036$) and lower blood pressures during tilt, but the groups did not differ in blood pressures during supine rest.

The LBD+ group had lower initial mean values for 2 indices of baroreflex-sympathoneural function—the log of the baroreflex area in Phase III of the Valsalva maneuver ($p=0.00721$) and the log of the pressure recovery time ($p=0.00467$). The groups did not differ in mean values for 2 indices of baroreflex-cardiovagal function—the baroslope during Phase II of the Valsalva maneuver (44) and $\Delta HR/\Delta BPs$ (45) during head-up tilt. The groups also did not differ in indices of heart rate variability in either the time or frequency domain.

Individual cases

Pure autonomic failure (PAF) evolving to DLB and PD+OH (LBD+ #8, Figure 9)

One of the LBD+ participants had comprehensive serial testing during life and at autopsy had tissues harvested for post-mortem neurochemical and neuropathologic analyses (Figure 9). This case has been described previously (10). Aspects relevant to the PDRisk study are presented here.

In the setting of a long history of post-traumatic stress disorder and dream enactment behavior, the participant developed OH, erectile dysfunction, and fatigue at about 67 years old. Three years later, he was diagnosed with PAF based on neurogenic OH and neuroimaging evidence of cardiac sympathetic denervation. He first reported visual hallucinations at age 72, and this problem persisted throughout the remainder of the clinical course. He had progressive cognitive decline (Montreal Cognitive Assessment (MoCA) score=22 at age 75 years, 18 at age 78 years) associated with obvious magnetic resonance image evidence of enlargement of the

lateral ventricles and diffuse cortical atrophy. He had gradually progressive parkinsonism (Unified Parkinson Disease Rating Scale (UPDRS) score of 27 at age 76 years old, 67 at 78 years old). University of Pennsylvania Smell Identification Test (UPSIT) scores at 70, 72, 73, and 78 years old indicated anosmia. He died at 79 years old with a diagnosis of DLB and PD+OH. Cardiac ^{18}F-dopamine PET at 70, 72, 73, 76, and 78 years showed persistently decreased ^{18}F-dopamine-derived radioactivity diffusely in the left ventricular myocardium. Immunoreactive αS was noted in sympathetic noradrenergic fibers in a skin biopsy (Figure 9D).

At the time of initial evaluation at 70 years old and 2 years later, the PUT/OCC ratios of ^{18}F-DOPA-derived radioactivity and washout percents of putamen ^{18}F-DOPA-derived radioactivity were normal. The first neuroimaging evidence of putamen dopamine deficiency was at 73 years old. Low PUT/OCC ratios were found in 2 subsequent scans at ages 76 and 78 years old (Figure 9C).

Autopsy revealed brainstem LBs without cortical LBs, decreased putamen dopamine content, and markedly decreased myocardial norepinephrine content. There were abundant αS-containing fibrils and severely decreased immunoreactive tyrosine hydroxylase (TH) in the sympathetic chain (Figure 9E).

PAF with glucocerebrosidase (GBA) gene mutation evolving to PD+OH (LBD+ #7, Figure 10)

A female participant reported OH, fainting, and dream enactment behavior beginning when she was about 38 years old. During her initial evaluation at the NIH Clinical Center, at age 57, cardiac ^{18}F-dopamine PET showed decreased radioactivity diffusely in the left ventricular myocardium, and she was diagnosed with PAF. This PET abnormality persisted in 4 subsequent ^{18}F-dopamine scans at ages 59, 60, 61, 63, and 65. UPSIT scores at 58, 61, 63, and 65 years old showed anosmia. Genetic testing revealed that she was a carrier for N370S mutation of the gene encoding glucocerebrosidase. Multi-tracer neuroimaging revealed greater loss of ^{18}F-dopamine- than of ^{11}C-methylreboxetine-derived radioactivity in the left ventricular myocardium (Figure 10A), demonstrating a vesicular storage defect in residual cardiac sympathetic nerves.

Two ^{18}F-DOPA PET scans (at 57 and 59 years old) were normal. The first evidence of a ^{18}F-DOPA PET abnormality occurred at 60 years old, 3 years after the first abnormal cardiac ^{18}F-dopamine PET scan. Visual hallucinations began at 59 years old and persisted subsequently. At 65, her UPDRS motor score was 58, and she was diagnosed with PD+OH. She did not have cognitive dysfunction as indicated by normal MoCA scores. Skin biopsy revealed increased αS-TH colocalization (Figure 9D). As of this writing, she is alive and carries a diagnosis of PD+OH.

Neurogenic OH with intact cardiac sympathetic innervation evolving to MSA (LBD- #20)

This female participant had a positive family history (father with PD), dream enactment behavior (RBD diagnosed by polysomnography), chronic constipation, urinary incontinence, heat intolerance, and orthostatic, post-prandial, and post-exertional dizziness. Upon initial evaluation she had OH (supine BP 164/90 mmHg, head-up tilt BP 92/65 mmHg, tilting stopped at 2' for safety reasons) that was determined to be neurogenic based on abnormal BP responses to the Valsalva maneuver. Her UPSIT score was 40, indicating normal sense of smell. The initial PUT/OCC ratio of ^{18}F-DOPA-derived radioactivity was decreased at 2.49.

At 4.6 years of follow-up (age 60.9 years old) she was diagnosed with PD by the blinded neurologist (GL). At the time of diagnosis, baroreflex-cardiovagal gain from Phase II continuous finger cuff BP data during the Valsalva maneuver was severely decreased at 0.87 ms/mmHg; (44) low frequency power of heart rate variability was low at 22 ms^2 (46), the orthostatic increment in plasma norepinephrine was attenuated (47%, normal ≥ 60%); and the pressure recovery time after release of the Valsalva maneuver was prolonged at 21.2 s (normal ≤ 5 s) (47), findings indicating combined baroreflex-cardiovagal and baroreflex-sympathoneural failure.

In this patient, cardiac ^{18}F-dopamine-derived radioactivity was consistently normal, both upon initial evaluation and across follow-up testing at 1.6, 3.4, and 4.6 years. Her UPSIT scores were also normal at these time points. The patient died in August 2021 at 64 years old. According to the Certificate of Death from the Vital Records Department of her county of residence, she died of MSA. There was no autopsy.

Concurrent loss of myocardial ^{18}F-dopamine-derived and putamen ^{18}F-DOPA-derived radioactivity (LBD+ #1, Figure 11)

This 59-year-old man of Austrian, Russian, Ukrainian, and Ashkenazic descent had a family history of PD, loss of sense of smell for about 5 years, and dream enactment behavior. A few months before the screening evaluation he was seen by a sleep specialist, who diagnosed RBD. Arm rigidity was noted, and the participant was referred to a movement disorder specialist, who found no evidence of PD about 2 months before the initial evaluation at the NIH. The participant was taking rasagiline once daily and clonazepam and melatonin at bedtime. The UPSIT score of 12/40 documented anosmia. The UPDRS score was 14/176. The initial PUT/OCC ratio of ^{18}F-DOPA-derived radioactivity was normal at 3.26, although the posterior/anterior ratio of radioactivity was low at 0.59 (arrow in Figure 11B) (48). ^{18}F-Dopamine-derived radioactivity was normal, with a normal rate of decline in radioactivity from the peak value.

At 1.6 years of follow-up the patient complained of limb rigidity, slowed movement (especially upon initiation of movement), bilateral resting tremor of the hands (more prominent in the right hand, worse with emotional agitation), slowed verbal expressiveness, decreased attentiveness and short-term memory, and micrographia. His medication regimen was the same. He was still anosmic (UPSIT score 14/40), but now his UPDRS score was 34/176, indicating mild parkinsonism, and the blinded neurologist diagnosed PD. The patient had a decreased PUT/OCC ratio (2.36) and increased washout of putamen ^{18}F-DOPA-derived radioactivity (23%).

After reaching the endpoint for participation in the PDRisk study, at 2.2 years from accrual into the study the patient returned for ^{18}F-dopamine PET under another protocol (NIH Clinical Protocol 03N0004) as a PD patient without OH. The entire time-activity curve for septal ^{18}F-dopamine-derived radioactivity was now shifted downward from the initial evaluation (Figure 11C, black squares), although the values at all time points were still within the normal range.

Apical and free wall ^{18}F-dopamine-derived radioactivity were now low at 5,719 and 4,674 nCi-kg/cc-mCi (Figure 11A). ^{13}N-Ammonia-derived radioactivity was unchanged (Figure 11D).

In summary, in this participant with preclinical PD serial ^{18}F-dopamine and ^{18}F-DOPA PET indicated approximately concurrent initial loss of apical and inferolateral left ventricular ^{18}F-dopamine-derived radioactivity and of posterior putamen ^{18}F-DOPA-derived radioactivity.

DISCUSSION

The results of the prospective, observational, long-term PDRisk study highlight the remarkable power of [18]F-dopamine PET for identifying preclinical central LBDs (PD or DLB) in at-risk individuals. The main finding is that among individuals with multiple PD risk factors (genetics, olfactory dysfunction, dream enactment, orthostatic intolerance), low cardiac [18]F-dopamine-derived radioactivity highly efficiently predicts the subsequent diagnosis of a central LBD.

In the overall PDRisk cohort of subjects with ≥3 risk factors, 26% were diagnosed with a central LBD during follow-up of up to about 7.5 years, a larger percentage than would be expected in the general population (49, 50). These data confirm the potency of the chosen combination of risk factors. Low [18]F-dopamine-derived radioactivity increased to a virtual certainty the likelihood of developing a central LBD. Meanwhile, neuroimaging evidence of intact cardiac noradrenergic innervation decreased to near zero the likelihood of a subsequent central LBD during follow-up, despite the same risk factors.

Persistent abnormalities of cardiac sympathetic innervation in preclinical central LBDs

Serial [18]F-dopamine PET enabled a determination as to whether cardiac [18]F-dopamine-derived radioactivity changed over years in the LBD+ or LBD- groups. There were no temporal trends in radioactivity in either group. Almost all the LBD+ participants already had low radioactivity upon initial evaluation, and almost all the LBD- participants had normal radioactivity throughout the period of follow-up. These findings indicate that cardiac noradrenergic deficiency was already advanced in most of the LBD+ group even upon initial evaluation.

The data do not address the time course for development of cardiac noradrenergic deficiency, with one exception. An LBD+ participant (LBD+ #1) seemed to be "caught in a window in time," in that initial interventricular septal cardiac [18]F-dopamine-derived radioactivity was normal, although apical radioactivity was decreased. About 2 years later, when the participant reached the study endpoint by being diagnosed with PD, apical and free wall

radioactivity were decreased, and the time-activity curve for septal radioactivity was shifted downward (Figure 11C). This is the typical pattern of regional progression of cardiac sympathetic denervation in PD without OH (51). Counting this individual, all the at-risk participants in the PDRisk study who were diagnosed with a central LBD during follow-up had evidence of antecedent cardiac noradrenergic deficiency by [18]F-dopamine PET.

The results in this patient suggest that once cardiac noradrenergic deficiency begins it progresses rapidly. Consistent with this view, we previously reported the case of a patient who had early onset PD and normal cardiac [18]F-dopamine-derived radioactivity for about 8 years; then free wall radioactivity declined, followed by decreased septal radioactivity 2 years later (35).

When does cardiac noradrenergic deficiency occur with respect to central dopaminergic deficiency in central LBDs?

Among the 9 subjects in the LBD+ group, 4 had normal initial PUT/OCC ratios of [18]F-DOPA-derived radioactivity, and 4 had normal initial washout percents of putamen [18]F-DOPA-derived radioactivity. During follow-up, the PUT/OCC ratios decreased and washout percents increased, whereas there were no trends in either biomarker in the LBD- group. In 3 of the 4 LBD+ individuals with normal initial PUT/OCC ratios, by the time of diagnosis the ratios were below the cutoff value; and in 3 of the 4 LBD+ individuals with normal initial washout percents, by the time of diagnosis the washout percents were above the cutoff value.

Since upon initial evaluation all the participants in the LBD+ group had evidence of diffuse or localized noradrenergic deficiency in the left ventricular myocardium, these findings indicate that the LBD+ group included a substantial subgroup in whom cardiac noradrenergic deficiency preceded putamen dopamine deficiency. This view fits with previous case reports describing low cardiac [18]F-dopamine-derived radioactivity before clinical or neuroimaging manifestations of PD (9) or DLB (10).

Combination of denervation with a vesicular storage defect in preclinical central LBDs

Interventricular septal [18]F-dopamine-derived radioactivity was significantly lower in the

LBD+ than in the LBD- and HV groups at all time points after and even during the 3-minute infusion of the tracer. Decreased uptake of ^{18}F-dopamine in the LBD+ group could not be attributed to decreased coronary perfusion, as the LBD+ and LBD- groups had similar time-activity curves for ^{13}N-ammonia derived radioactivity.

A particular functional abnormality in residual cardiac sympathetic nerves—inefficient vesicular sequestration of catecholamines—was associated with an increased probability of subsequently developing a central LBD. The area under the ROC curve for $k_{Max\text{-}25}$, in the LBD+ and LBD- groups (0.92) indicated excellent ability of this functional biomarker for distinguishing the two groups, with sensitivity 89% at specificity 96% by Youden's method. Denervation alone cannot explain accelerated loss of ^{18}F-dopamine-derived radioactivity (42).

The breakpoint analyses showed that individuals with preclinical central LBDs had at least some degree of cardiac sympathetic denervation. If there were only a vesicular storage defect, without denervation, then the rate of increase in radioactivity between 3' and peak radioactivity would be attenuated in the LBD+ group, and this was not the case. The LBD+ group also had at least some degree of a vesicular storage defect, because if there were only a loss of sympathetic nerves, with normal vesicular function in the residual terminals, then the rate of decrease in radioactivity from the peak value to 13' would be normal, and this also was not the case. From the breakpoint analyses we therefore infer that low cardiac ^{18}F-dopamine-derived radioactivity in the LBD+ group reflected a combination of denervation with a vesicular storage defect in residual sympathetic nerves. The data confirm predictions from computational modeling as applied to intra-neuronal determinants of norepinephrine stores in cardiac sympathetic nerves in LBDs (5).

The LBD+ group had increased washout percents of putamen ^{18}F-DOPA-derived radioactivity, consistent with the view that decreased vesicular storage in catecholaminergic neurons also occurs in the nigrostriatal dopaminergic system (52). Post-mortem neurochemistry has confirmed the occurrence of a vesicular storage defect both in the heart (53) and in the putamen (54) in LBDs. The latter has also been demonstrated directly in isolated striatal vesicles

from PD patients (41).

Pure autonomic failure may be a prototype of "body-first" central LBDs

Two of the LBD+ participants (LBD+ #7 and LBD+ #8) had PAF, a rare disease characterized by neurogenic OH, generalized sympathetic noradrenergic deficiency, and intra-neuronal deposition of αS in skin biopsies (55), without clinical evidence of motor or cognitive impairment. Although patients with clinically diagnosed PAF can go on for many years without evincing symptoms or signs of a central LBD (56), PAF can evolve to PD or DLB (9, 10, 23, 57), and post-mortem neuropathology has documented brainstem Lewy bodies in virtually all PAF patients (57).

Autopsy findings in a PAF patient in the LBD+ group (LBD #8) showed increased cardiac, brainstem, and sympathetic ganglionic αS deposition (Figure 9E). Prior to death, this patient had an elevated αS-TH colocalization index in a skin biopsy (Figure 9D). PUT/OCC ratios of [18]F-DOPA-derived radioactivity showed a tri-phasic downward trend over the years of follow-up (Figure 9C), mirroring the tri-phasic pattern found in cardiac norepinephrine stores in LBDs (35). Based on this tri-phasic pattern we propose that a transition from normal to rapid decline in PUT/OCC ratios may identify the optimal time for initiation of treatment targeting the vesicular storage defect in striatal dopaminergic terminals. In the LBD- group, however, there was substantial variability over time in values for both cardiac [18]F-dopamine-derived radioactivity (Figure 5B) and PUT/OCC ratios of [18]F-DOPA-derived radioactivity (Figure 8A), meaning that it may take years of follow-up for a clear downward trend to be recognized.

Central and peripheral non-motor aspects of LBDs are correlated with each other

RBD is a strong risk factor for subsequent development of a neurodegenerative synucleinopathy (58), including a "diffuse/malignant" form of PD (59) that features OH (60, 61). RBD is also associated with olfactory dysfunction (62, 63) and neuroimaging evidence of cardiac noradrenergic deficiency (64). Longitudinal studies of RBD patients have led to the view that autonomic dysfunction can occur early in neurodegenerative synucleinopathies, years before the motor or cognitive onset of central LBDs (22). The present data fit with substantial overlaps

among dream enactment behavior, olfactory dysfunction, OH, and cardiac noradrenergic deficiency in preclinical central LBDs.

Evolution to MSA

One PDRisk study participant with neurogenic OH (LBD- #20) had persistently normal [18]F-dopamine-derived radioactivity and normal scores on the UPSIT, findings that argue strongly against PD+OH (52, 65). The patient was diagnosed with PD by the blinded neurologist. A few years after reaching the study endpoint, the patient died. According to the obituary and the official Certificate of Death, the cause of death was MSA. This case seems to be an exception that proves the rule. Even an expert movement disorders neurologist may not be able to distinguish PD+OH from the parkinsonian form of MSA by clinical examination alone; however, consistently normal [18]F-dopamine-derived radioactivity rules out PD+OH (66).

Where in the autonomic nervous system do central LBDs begin?

The present results support the view that the pathogenetic process leading to central LBDs often begins outside the brain, in the autonomic nervous system. Much recent attention has focused on the possibility of early synucleinopathy in the gut, followed by trans-synaptic retrograde transmission of αS via the vagus nerve to the dorsal motor nucleus of the vagus in the caudal medulla (67-69). How synucleinopathy in the enteric nervous system, in vagal nerve fibers, in myocardium, and in sympathetic noradrenergic axons in skin biopsies (70) are related remains poorly understood.

Catecholamines are not only neurotransmitters but also hormones (epinephrine being the archetype) and autocrine-paracrine factors (exemplified by renal dopamine) (71, 72). Most of the synthesis and metabolism of catecholamines in the human body take place not in the brain or autonomic nerves but in the gut (73, 74). Since all of the intracellular metabolism of dopamine passes through 3,4-dihydroxyphenylacetaldehyde (DOPAL), which potently oligomerizes, quinonizes, and aggregates αS (75, 76), it seems reasonable to speculate that catecholaldehyde-αS interactions in the gut constitute an early pathogenetic mechanism in LBDs (36). Thus, in animals, DOPAL injection into the vagus nerve augments axonal transport of toxic αS oligomers

(77) to both the brainstem and heart.

Study Limitations

The PDRisk study involved a relatively small number of subjects. This was because of the strong hypothesis and the power calculation when the study was designed. It was unnecessary and possibly ethically questionable to conduct comprehensive, multi-modality clinical laboratory assessments involving more than minimal risk in larger cohorts repeatedly over a substantial number of years. We believe that the fact that the results from applying different testing approaches agreed with each other reinforce the validity of the conclusions by consilience (78).

Since all the PDRisk subjects had multiple risk factors, generalizability to people with fewer or different risk factors could not be determined.

[18]F-Dopamine PET is only available at the NIH Clinical Center. We hope that the extraordinary results reported here documenting the ability to identify preclinical central LBDs will induce researchers at other institutions to join the Investigational New Drug (IND) application for [18]F-dopamine (IND #33,866), which has been active for more than 30 years, or apply for an IND, about which we would be happy to advise or collaborate. This technology should be applied in larger populations of less stringently selected at-risk individuals, a type of study that cannot be done solely within intramural NIH. One might consider [123]I-metaiodobenzylguanidine ([123]I-MIBG) single photon emission computed tomography (SPECT), which is available at most centers for diagnostic evaluation of pheochromocytoma, but insurance carriers in the United States do not cover [123]I-MIBG SPECT in known or suspected LBDs. We have commented about this for many years (79, 80).

Implications

The present results have clear implications for treatment and prevention trials for individuals at high risk of central LBDs. Biomarkers of cardiac noradrenergic deficiency seem to identify a disease process that will progress to a central LBD. Assessing these biomarkers in at-risk individuals may be valuable both for efficient selection of eligible candidates and for assessing effects of potential neurorescue or neuroprotective approaches objectively and

quantitatively. Computational modeling indicates that strategies targeting toxic catecholaldehyde-αS interactions in catecholaminergic neurons would substantially delay the onset of symptomatic LBDs (35). We propose that a clinical trial involving a relatively small number of highly selected participants should enable testing for the first time of whether central LBDs can be prevented in at-risk individuals.

METHODS

Study approval

The Institutional Review Board (IRB) of the National Institute of Neurological Disorders and Stroke (NINDS) approved the PDRisk study in 2009. The study was conducted under National Institutes of Health (NIH) Clinical Protocol 09N0010, "Biomarkers of Risk of Parkinson Disease." The setting was the NIH Clinical Center.

Recruitment

Recruitment into the PDRisk study was via an IRB-approved Google ad that directed visitors to an IRB-approved, protocol-specific, secure website (https://PDRisk.ninds.nih.gov, now inactive). Visitors interested in registering for the study were given confidential, unique identification numbers via email. After consenting to the study electronically in a manner compliant with the Privacy Rule (45 CFR 164.501, 164.508, 164.512(i)), participants were queried about 4 types of risk factor—genetic, olfactory, dream enactment behavior, and orthostatic hypotension (OH) or intolerance. Candidate participants who reported at least 3 risk factors at the website were interviewed by phone by a Research Nurse to confirm the self-reported information and select subjects for on-site screening.

Inclusion and exclusion criteria

Eligibility criteria for the PDRisk study included a participant age of 18 years old or older. A candidate participant was excluded if there were any disqualifying medical conditions (e.g., insulin-dependent diabetes mellitus, symptomatic cerebrovascular or coronary heart disease, renal failure), PD had already been diagnosed, the registrant was more than 70 years old, or clinical considerations required continued treatment with a drug likely to interfere with the scientific results (website http://clinicalstudies.info.nih.gov/cgi/detail.cgi?A_2009-N-0010.html#eligibility). Recruitment was done independently of sex, gender, race, ethnicity, or national origin.

Screening examination

The purposes of the on-site screening examination at the NIH Clinical Center were to

obtain consent for further participation in the study, verify at least 3 risk factors, and perform clinical laboratory tests as described below.

A positive family history (≥ 1 first-degree relative or ≥ 2 second-degree relatives with PD) confirmed at the time of on-site screening at the NIH Clinical Center satisfied the genetic criterion. Decreased sense of smell reported at the protocol-specific website and verified by the University of Pennsylvania Smell Identification test (moderate or severe microsmia or anosmia) (81) satisfied the olfactory criterion. To satisfy the dream enactment risk factor criterion, the individual or member of the individual's household must have reported that the individual had movements of the body or limbs associated with dreaming and at least one of the following: potentially harmful sleep behavior, dreams that appeared to be acted out, and sleep behavior that disrupted sleep continuity (82). A polysomnographic diagnosis of RBD was not required. To satisfy the OH risk factor criterion, the individual must have reported symptoms of OH or having OH, corroborated at the screening evaluation.

Subjects with ≥ 3 confirmed risk factors underwent inpatient biomarkers testing and follow-up over 5 1.5-year intervals (total 7.5 years) or until diagnosed with PD.

Outcome measures

The primary outcome measure was a diagnosis of PD by a neurologist who was blinded as to the results of the biomarkers testing. PD was diagnosed according to accepted clinical criteria such as bradykinesia, rigidity, resting tremor, and imbalance. DLB was diagnosed based on cognitive dysfunction, parkinsonism, and two other core features—visual hallucinations and fluctuating attention and concentration (83, 84). A diagnosis of DLB was not designed in as an outcome measure.

Study sample size

The PDRisk study had a strong primary hypothesis, which was that among at-risk individuals, positive biomarkers of catecholaminergic neurodegeneration in the heart or brain identify pre-motor PD. To estimate the required numbers of subjects we used a log-rank test for evaluating the association between biomarkers and LBD+ diagnosis, and predicted that among

individuals who were at risk of PD *and* had abnormal catecholaminergic biomarkers, 80% would develop LBD+ by 7.5 years of follow-up; and that among at-risk participants without abnormal biomarkers, 20% would develop LBD+ during follow-up. Power analysis indicated that 26 participants would be sufficient (24, 48) to detect the association at an alpha value of 0.05 and beta value of 0.20.

Study groups

The PDRisk study cohort was stratified into 3 groups—a group that during follow-up was diagnosed with a central LBD (LBD+); a group that during follow-up was not diagnosed with a central LBD (LBD-); and a group that upon screening evaluation did not have at least 3 confirmed risk factors and was not invited to return for follow-up testing (PDRisk-). For comparison purposes, a concurrent control group of age-matched HVs was included.

Dynamic ^{18}F-dopamine PET

In the PDRisk study dynamic PET images were obtained in 5 1-minute frames, then 3 5-minute frames (midpoints about 8, 13, and 18 minutes, and a final 10' frame with midpoint 25' from the time of initiation of the infusion.

The main outcome measurement variable was the amount of ^{18}F-dopamine-derived radioactivity during the 5-minute frame with midpoint about 8' from initiation of tracer administration, as we have used this variable in several previous studies.(24, 35, 46, 52, 66, 85, 86) Other outcome measurement variables were the amount of radioactivity in the frame when the infusion ended (midpoint 3' from initiation of tracer administration), radioactivity in the last dynamic frame (midpoint about 25'), maximum radioactivity, the slope of mono-exponential decline in radioactivity from the maximum radioactivity to 25' ($k_{Max\text{-}25'}$) in units of min^{-1} and the area under the time-activity curve (Area TAC) for radioactivity across the 9 dynamic frames, calculated based on the trapezoidal rule. The values for Area TAC were standardized by dividing by 25', the midpoint of the last scanning frame.

Neurochemical and neuroimaging indices of central dopamine deficiency

Most of the PDRisk+ participants underwent both lumbar puncture for assays of CSF levels

of catechols and brain ^{18}F-DOPA PET, by methods described previously by our group (48). Briefly, lumbar puncture was done under fluoroscopic guidance. One-cc aliquots of CSF were frozen immediately on dry ice and kept frozen at -80 ^{o}C until assayed for catechols by batch alumina extraction followed by liquid chromatography with series electrochemical detection. For ^{18}F-DOPA PET, 7 mCi of the tracer was administered intravenously without carbidopa pretreatment. A static 15' emission scan was obtained beginning at 30' after tracer administration, and a static 15' emission scan was obtained ending at 120' after tracer administration. The putamen/occipital cortex (PUT/OCC) ratio of ^{18}F-DOPA-derived radioactivity was calculated for the second emission scan (52). The percent washout of radioactivity was calculated from the PUT radioactivity in the first scan minutes the radioactivity in the second scan, the quantity divided by the radioactivity in the first scan.

Autonomic function testing

Autonomic function testing in the LBD+, LBD-, and PDRisk- groups included measures of heart rate variability in the time and frequency domains during supine rest (46), beat-to-beat finger blood pressure and heart rate responses to the Valsalva maneuver (31), and hemodynamic and plasma catechol responses to head-up tilt table testing for 5 minutes at 90 degrees from horizontal (32, 33).

Efforts to reduce bias

Determinations of eligibility for the study at the PDRisk webpage were done using a computer algorithm without regard to sex, gender, race, or ethnicity. For the primary outcome measure, a neurologist who was blinded as to the reported biomarkers examined each participant at each follow-up visit and rendered a decision about whether the participant had PD, with a written consult note entered into the Clinical Research Information System. The personnel who analyzed the PET images, performed neurochemical assays, and conducted immunofluorescence confocal microscopy were blinded as to the identity of the participants until the data were tabulated in spreadsheets.

Data analysis and statistics

Normality assumption testing and outlier identification were based on the studentized residuals. All p-values were two-tailed. The statistical significance level was set at α=0.05, since there was one primary outcome (LBD+ diagnosis) and one primary biomarker (septal [18]F-dopamine-derived radioactivity in the dynamic PET frame with midpoint 8'). The statistical analyses were performed using SAS version 9.4 (SAS Institute, Cary, NC), GraphPad Prism 9.3 for Mac OS (GraphPad, San Diego, CA), and KaleidaGraph 5.0 (Synergy Software, Reading, PA). Statistical testing was done to answer the following questions.

(1) Does low [18]F-dopamine-derived radioactivity increase the likelihood of a subsequent diagnosis of a central LBD?

The survival time was defined as the follow-up years from the first visit date to the date when a central LBD was diagnosed, where all subjects without LBD+ (including the patients who were lost to follow-up) were treated as censored. [18]F-Dopamine-derived radioactivity in the interventricular septum in the dynamic frame with midpoint about 8' from initiation of tracer administration was dichotomized as low vs. normal using a threshold of 6,000 nCi-kg/cc-mCi, which was based on the first look at the data (24). The comparison in the time to LBD+ diagnosis between low and normal groups was performed using the Kaplan-Meier survival curve and log-rank test.

(2) Do LBD+ and LBD- groups differ in terms of initial [18]F-dopamine-derived radioactivity?

For each of the 6 biomarkers of [18]F-dopamine PET at the time of initial evaluation, analysis of covariance (ANCOVA) with age and sex considered as covariates was applied to compare the means among subject groups (LBD+, LBD-, or HV). Tukey's method was used in the pairwise multiple comparisons.

(3) How well does low initial [18]F-dopamine-derived radioactivity separate the LBD+ and LBD- groups?

For each of the 6 initial [18]F-dopamine PET variables, receiver operating characteristic (ROC) curve analysis was used to assess the separability between the LBD+ and LBD- groups. In general, the area under the ROC curve (AUC) values are considered excellent (≥0.90), good

(AUC 0.80-0.90), fair (0.70-0.80), or poor (<0.70). Sensitivity and specificity for each biomarker were estimated based on the optimal threshold chosen using the Youden method.

(4) Does cardiac [18]F-dopamine-derived radioactivity change during long-term follow-up in the LBD+ or LBD- groups?

To examine the change in cardiac [18]F-dopamine-derived radioactivity during follow-up in the LBD+ and LBD- groups, a linear random coefficient model (Littell et al. 1996) was used. The model was applied to evaluate the change in 8' radioactivity over time (follow-up years), where the intercept and slope were random effects, and age and sex were considered the covariates. The linear model included time (follow-up years), group (LBD+, LBD-), and interaction between time and group. The interaction test was used to examine the slope homogeneity between the two groups.

(5) Do LBD+ and LBD- participant groups differ in terms of the uptake or subsequent loss of septal [18]F-dopamine-derived radioactivity within the initial PET session?

A piecewise linear random coefficient model (87, 88) was used to examine the rapid increase and slow subsequent loss of [18]F-dopamine-derived radioactivity in the LBD+, LBD- and HV groups. The model with one breakpoint (representing two linear lines with different slopes) was applied to evaluate the difference in slope between the three groups (SAS procedure MIXED), where the intercept, the slope of the first linear line, and the difference in slope between the two linear lines were treated as random effects, and the covariance structure (3x3) was specified as unstructured.

(6) Are the 6 measures of [18]F-dopamine-derived radioactivity and the 3 indices of central dopaminergic innervation correlated?

Pearson and Spearman correlation coefficients were used to evaluate the relationship among the 6 biomarkers of dynamic [18]F-dopamine PET and three biomarkers of central dopamine deficiency.

(7) Do the LBD+ and LBD- groups differ in terms of indices of central dopaminergic innervation or function upon initial evaluation? Analysis of variance (with multiple

comparisons) among the LBD+, LBD-, and HV groups was conducted on data for CSF 3,4-dihydroxyphenylacetic acid (DOPAC) levels (48), the putamen/occipital cortex (PUT/OCC) ratio of [18]F-DOPA-derived radioactivity in the 15'-minute static emission scan ending 2 hours after tracer administration (52), and the percent decline in radioactivity between the first (beginning about 30' after tracer injection) and second (ending about 120' after tracer injection) 15'-minute static emission scans (52).

(8) Does the LBD+ group differ from the LBD- groups in terms of physiological or neurochemical autonomic functions upon initial evaluation? Two-sample t tests were conducted comparing the LBD+ and LBD- groups with particular attention to heart rate variability in the time and frequency domains, baroreflex-sympathoneural and baroreflex-cardiovagal function, and hemodynamic and plasma norepinephrine responses to head-up tilt.

The main autonomic function variables for heart rate variability in the time domain were the interbeat interval (normalized by exclusion of ectopic beats or artifacts (NN)), the standard deviation of the NN interval, and the coefficient of variation of the NN interval. In the frequency domain the data were for low frequency (LF) power, high frequency (HF) power, normalized LF and HF power (LFnu, HFnu), and the LF/HF ratio (46).

Baroreflex-cardiovagal function was quantified by the slope of the relationship between cardiac interbeat interval and systolic blood pressure during Phase II of the Valsalva maneuver(31) and by the magnitude of increase in heart rate for a given decrease in systolic pressure during head-up tilt.(45) Baroreflex-sympathoneural function was quantified by the log of the baroreflex area in Phase III after release of the Valsalva maneuver(89) and the log of the pressure recovery time (PRT) (31).

AUTHOR CONTRIBUTIONS:

DSG: design of the research study, conducting procedures, data acquisition, data analysis, manuscript writing, figures and tables, manuscript editing

CH: imaging data acquisition, tabulation, and analysis

PS: biochemical data acquisition, data analysis, manuscript editing

GL: neurological examinations, data acquisition, data analysis, manuscript editing

JG: patient care coordination, conducting procedures, data acquisition, data analysis

SM: conducting procedures, demographic and clinical data acquisition, data analysis

RI: data acquisition, data analysis, manuscript editing

TW: statistical methods, data analysis, manuscript writing, figures and tables, manuscript editing

YS: study conception and design, manuscript editing

ACKNOWLEDGEMENTS: The Division of Intramural Research, NINDS, NIH supported the research reported here. We gratefully acknowledge the assistance of the NIH PET Department.

REFERENCES

1. Kim JS, Park HE, Oh YS, Song IU, Yang DW, Park JW, et al. (123)I-MIBG myocardial scintigraphy and neurocirculatory abnormalities in patients with dementia with Lewy bodies and Alzheimer's disease. J Neurol Sci. 2015;357(1-2):173-7.
2. Yoshita M, Arai H, Arai H, Arai T, Asada T, Fujishiro H, et al. Diagnostic accuracy of 123I-meta-iodobenzylguanidine myocardial scintigraphy in dementia with Lewy bodies: a multicenter study. PLoS One. 2015;10(3):e0120540.
3. Orimo S, Amino T, Itoh Y, Takahashi A, Kojo T, Uchihara T, et al. Cardiac sympathetic denervation precedes neuronal loss in the sympathetic ganglia in Lewy body disease. Acta Neuropathol. 2005;109(6):583-8.
4. Isonaka R, Sullivan P, and Goldstein DS. Pathophysiological significance of increased alpha-synuclein deposition in sympathetic nerves in Parkinson's disease: a post-mortem observational study. Transl Neurodegener. 2022;11(1):15.
5. Goldstein DS, Pekker MJ, Eisenhofer G, and Sharabi Y. Computational modeling reveals multiple abnormalities of myocardial noradrenergic function in Lewy body diseases. JCI Insight. 2019;5; (16):e130441.
6. Kish SJ, Shannak K, and Hornykiewicz O. Uneven pattern of dopamine loss in the striatum of patients with idiopathic Parkinson's disease. Pathophysiologic and clinical implications. The New England Journal of Medicine. 1988;318:876-80.
7. Kashihara K, Ohno M, Kawada S, and Okumura Y. Reduced cardiac uptake and enhanced washout of 123I-MIBG in pure autonomic failure occurs conjointly with Parkinson's disease and dementia with Lewy bodies. J Nucl Med. 2006;47(7):1099-101.
8. Yoshita M, Taki J, Yokoyama K, Noguchi-Shinohara M, Matsumoto Y, Nakajima K, et al. Value of 123I-MIBG radioactivity in the differential diagnosis of DLB from AD. Neurology. 2006;66(12):1850-4.
9. Goldstein DS, Sharabi Y, Karp BI, Bentho O, Saleem A, Pacak K, et al. Cardiac sympathetic denervation preceding motor signs in Parkinson disease. Clin Auton Res.

2007;17(2):118-21.

10. Goldstein DS, Holmes C, Sewell L, Park MY, and Sharabi Y. Sympathetic noradrenergic before striatal dopaminergic denervation: relevance to Braak staging of synucleinopathy. Clin Auton Res. 2012;22(1):57-61.
11. Del Tredici K, Hawkes CH, Ghebremedhin E, and Braak H. Lewy pathology in the submandibular gland of individuals with incidental Lewy body disease and sporadic Parkinson's disease. Acta Neuropathol. 2010;119(6):703-13.
12. Ghebremedhin E, Del Tredici K, Langston JW, and Braak H. Diminished tyrosine hydroxylase immunoreactivity in the cardiac conduction system and myocardium in Parkinson's disease: an anatomical study. Acta Neuropathol. 2009;118(6):777-84.
13. Fujishiro H, Frigerio R, Burnett M, Klos KJ, Josephs KA, Delledonne A, et al. Cardiac sympathetic denervation correlates with clinical and pathologic stages of Parkinson's disease. Mov Disord. 2008;23(8):1085-92.
14. Horsager J, Andersen KB, Knudsen K, Skjaerbaek C, Fedorova TD, Okkels N, et al. Brain-first versus body-first Parkinson's disease: a multimodal imaging case-control study. Brain. 2020;143(10):3077-88.
15. Simon-Sanchez J, Schulte C, Bras JM, Sharma M, Gibbs JR, Berg D, et al. Genome-wide association study reveals genetic risk underlying Parkinson's disease. Nat Genet. 2009;41(12):1308-12.
16. Ponsen MM, Stoffers D, Booij J, van Eck-Smit BL, Wolters E, and Berendse HW. Idiopathic hyposmia as a preclinical sign of Parkinson's disease. Ann Neurol. 2004;56(2):173-81.
17. Doppler K, Jentschke HM, Schulmeyer L, Vadasz D, Janzen A, Luster M, et al. Dermal phospho-alpha-synuclein deposits confirm REM sleep behaviour disorder as prodromal Parkinson's disease. Acta Neuropathol. 2017;133(4):535-45.
18. Goldstein DS. Orthostatic hypotension as an early finding in Parkinson disease. Clin Auton Res. 2006;16:46-64.

19. Chia R, Sabir MS, Bandres-Ciga S, Saez-Atienzar S, Reynolds RH, Gustavsson E, et al. Genome sequencing analysis identifies new loci associated with Lewy body dementia and provides insights into its genetic architecture. Nat Genet. 2021;53(3):294-303.
20. Olichney JM, Murphy C, Hofstetter CR, Foster K, Hansen LA, Thal LJ, et al. Anosmia is very common in the Lewy body variant of Alzheimer's disease. JNeurol Neurosurg Psychiatry. 2005;76(10):1342-7.
21. Miyamoto T, and Miyamoto M. Phenoconversion from Idiopathic Rapid Eye Movement Sleep Behavior Disorder to Lewy Body Disease. Mov Disord Clin Pract. 2018;5(5):506-11.
22. Postuma RB, Gagnon JF, Pelletier A, and Montplaisir J. Prodromal autonomic symptoms and signs in Parkinson's disease and dementia with Lewy bodies. Mov Disord. 2013;28(5):597-604.
23. Kaufmann H, Norcliffe-Kaufmann L, Palma JA, Biaggioni I, Low PA, Singer W, et al. Natural history of pure autonomic failure: A United States prospective cohort. Ann Neurol. 2017;81(2):287-97.
24. Goldstein DS, Holmes C, Lopez GJ, Wu T, and Sharabi Y. Cardiac sympathetic denervation predicts PD in at-risk individuals. Parkinsonism Relat Disord. 2018;52:90-3.
25. Lamotte G, Holmes C, Sullivan P, Lenka A, and Goldstein DS. Cardioselective peripheral noradrenergic deficiency in Lewy body synucleinopathies. Ann Clin Transl Neurol. 2020;7(12):2450-60.
26. Leenders KL, Salmon EP, Tyrrell P, Perani D, Brooks DJ, Sager H, et al. The nigrostriatal dopaminergic system assessed in vivo by positron emission tomography in healthy volunteer subjects and patients with Parkinson's disease. Arch Neurol. 1990;47(12):1290-8.
27. Jokinen P, Helenius H, Rauhala E, Bruck A, Eskola O, and Rinne JO. Simple ratio analysis of 18F-fluorodopa uptake in striatal subregions separates patients with early Parkinson disease from healthy controls. J Nucl Med. 2009;50(6):893-9.
28. Ono SA, Sato T, and Muramatsu S. Freezing of Gait in Parkinson's Disease Is Associated with Reduced 6-[(18)F]Fluoro-l-m-tyrosine Uptake in the Locus Coeruleus. Parkinsons

Dis. 2016;2016:5430920.

29. Goldstein DS, Holmes C, Cannon RO, 3rd, Eisenhofer G, and Kopin IJ. Sympathetic cardioneuropathy in dysautonomias. N Engl J Med. 1997;336(10):696-702.
30. Goldstein DS, Sullivan P, Holmes C, Lamotte G, Lenka A, and Sharabi Y. Differential abnormalities of cerebrospinal fluid dopaminergic versus noradrenergic indices in synucleinopathies. J Neurochem. 2021;158(2):554-68.
31. Goldstein DS, and Cheshire WP, Jr. Beat-to-beat blood pressure and heart rate responses to the Valsalva maneuver. Clin Auton Res. 2017;27(6):361-7.
32. Cheshire WP, Jr., and Goldstein DS. Autonomic uprising: the tilt table test in autonomic medicine. Clin Auton Res. 2019;29(2):215-30.
33. Goldstein DS, and Cheshire WP. Roles of catechol neurochemistry in autonomic function testing. Clin Auton Res. 2018.
34. Goldstein DS. "Sick-but-not-dead": Multiple paths to catecholamine deficiency in Lewy Body diseases. Stress. 2020:1-16.
35. Goldstein DS, Pekker MJ, Sullivan P, Isonaka R, and Sharabi Y. Modeling the Progression of Cardiac Catecholamine Deficiency in Lewy Body Diseases. J Am Heart Assoc. 2022;11(11):e024411.
36. Masato A, Plotegher N, Terrin F, Sandre M, Faustini G, Thor A, et al. DOPAL initiates alphaSynuclein-dependent impaired proteostasis and degeneration of neuronal projections in Parkinson's disease. NPJ Parkinsons Dis. 2023;9(1):42.
37. Goldstein DS. The catecholaldehyde hypothesis: where MAO fits in. J Neural Transm. 2020;127(2):169-77.
38. Zhang S, Wang R, and Wang G. Impact of Dopamine Oxidation on Dopaminergic Neurodegeneration. ACS Chem Neurosci. 2019;10(2):945-53.
39. Landau R, Halperin R, Sullivan P, Zibly Z, Leibowitz A, Goldstein DS, et al. The rat rotenone model reproduces the abnormal pattern of central catecholamine metabolism found in Parkinson's disease. Dis Model Mech. 2022;15;doi10.1242/dmm.049082(1).

40. Plotegher N, Berti G, Ferrari E, Tessari I, Zanetti M, Lunelli L, et al. DOPAL derived alpha-synuclein oligomers impair synaptic vesicles physiological function. Sci Rep. 2017;7:40699.
41. Pifl C, Rajput A, Reither H, Blesa J, Cavada C, Obeso JA, et al. Is Parkinson's disease a vesicular dopamine storage disorder? Evidence from a study in isolated synaptic vesicles of human and nonhuman primate striatum. J Neurosci. 2014;34(24):8210-8.
42. Goldstein DS, Holmes C, Sullivan P, Mash DC, Sidransky E, Stefani A, et al. Deficient vesicular storage: A common theme in catecholaminergic neurodegeneration. Parkinsonism Relat Disord. 2015;21(9):1013-22.
43. Goldstein DS, Grossman E, Tamrat M, Chang PC, Eisenhofer G, Bacher J, et al. Positron emission imaging of cardiac sympathetic innervation and function using 18F-6-fluorodopamine: effects of chemical sympathectomy by 6-hydroxydopamine. J Hypertens. 1991;9:417-23.
44. Goldstein DS, Horwitz D, and Keiser HR. Comparison of techniques for measuring baroreflex sensitivity in man. Circulation. 1982;66:432-9.
45. Norcliffe-Kaufmann L, Kaufmann H, Palma JA, Shibao CA, Biaggioni I, Peltier AC, et al. Orthostatic heart rate changes in patients with autonomic failure caused by neurodegenerative synucleinopathies. Ann Neurol. 2018;83(3):522-31.
46. Goldstein DS, Bentho O, Park MY, and Sharabi Y. Low-frequency power of heart rate variability is not a measure of cardiac sympathetic tone but may be a measure of modulation of cardiac autonomic outflows by baroreflexes. Exp Physiol. 2011;96(12):1255-61.
47. Goldstein DS, and Sharabi Y. Baroreflex-sympathoneural dysfunction characterizes at-risk individuals with preclinical central Lewy body diseases. Clin Auton Res. 2022.
48. Goldstein DS, Holmes C, Lopez GJ, Wu T, and Sharabi Y. Cerebrospinal fluid biomarkers of central dopamine deficiency predict Parkinson's disease. Parkinsonism Relat Disord. 2018;50:108-12.

49. Savica R, Boeve BF, and Logroscino G. Epidemiology of alpha-synucleinopathies: from Parkinson disease to dementia with Lewy bodies. Handb Clin Neurol. 2016;138:153-8.
50. Muangpaisan W, Mathews A, Hori H, and Seidel D. A systematic review of the worldwide prevalence and incidence of Parkinson's disease. J Med Assoc Thai. 2011;94(6):749-55.
51. Li ST, Dendi R, Holmes C, and Goldstein DS. Progressive loss of cardiac sympathetic innervation in Parkinson's disease. Ann Neurol. 2002;52(2):220-3.
52. Goldstein DS, Holmes C, Bentho O, Sato T, Moak J, Sharabi Y, et al. Biomarkers to detect central dopamine deficiency and distinguish Parkinson disease from multiple system atrophy. Parkinsonism Relat Disord. 2008;14(8):600-7.
53. Goldstein DS, Sullivan P, Holmes C, Miller GW, Sharabi Y, and Kopin IJ. A vesicular sequestration to oxidative deamination shift in myocardial sympathetic nerves in Parkinson disease. J Neurochem. 2014;131:219-28.
54. Goldstein DS, Sullivan P, Holmes C, Kopin IJ, Basile MJ, and Mash DC. Catechols in post-mortem brain of patients with Parkinson disease. Eur J Neurol. 2011;18:703-10.
55. Donadio V, Incensi A, Cortelli P, Giannoccaro MP, Jaber MA, Baruzzi A, et al. Skin sympathetic fiber alpha-synuclein deposits: a potential biomarker for pure autonomic failure. Neurology. 2013;80(8):725-32.
56. Singer W, Berini SE, Sandroni P, Fealey RD, Coon EA, Suarez MD, et al. Pure autonomic failure: Predictors of conversion to clinical CNS involvement. Neurology. 2017;88(12):1129-36.
57. Goldstein DS, Isonaka R, Lamotte G, and Kaufmann H. Different phenoconversion pathways in pure autonomic failure with versus without Lewy bodies. Clin Auton Res. 2021;31(6):677-84.
58. Postuma RB, Iranzo A, Hogl B, Arnulf I, Ferini-Strambi L, Manni R, et al. Risk factors for neurodegeneration in idiopathic rapid eye movement sleep behavior disorder: a multicenter study. Ann Neurol. 2015;77(5):830-9.
59. Fereshtehnejad SM, Romenets SR, Anang JB, Latreille V, Gagnon JF, and Postuma RB.

New clinical subtypes of Parkinson disease and their longitudinal progression: A prospective cohort comparison with other phenotypes. JAMA Neurol. 2015;72(8):863-73.

60. Yin K, Zhou C, Zhu Y, Yin W, Yin L, Liu B, et al. REM sleep behavioral disorder may be an independent risk factor for orthostatic hypotension in Parkinson's disease. Aging Clin Exp Res. 2022;34(1):159-66.
61. Kim JS, Park HE, Oh YS, Lee SH, Park JW, Son BC, et al. Orthostatic hypotension and cardiac sympathetic denervation in Parkinson disease patients with REM sleep behavioral disorder. J Neurol Sci. 2016;362:59-63.
62. Fantini ML, Postuma RB, Montplaisir J, and Ferini-Strambi L. Olfactory deficit in idiopathic rapid eye movements sleep behavior disorder. Brain Res Bull. 2006;70(4-6):386-90.
63. Siderowf A, Jennings D, Eberly S, Oakes D, Hawkins KA, Ascherio A, et al. Impaired olfaction and other prodromal features in the Parkinson At-Risk Syndrome Study. Mov Disord. 2012;27(3):406-12.
64. Fedorova TD, Knudsen K, Andersen KB, Horsager J, Skjaerbaek C, Beier CP, et al. Imaging progressive peripheral and central dysfunction in isolated REM sleep behaviour disorder after 3 years of follow-up. Parkinsonism Relat Disord. 2022;101:99-104.
65. Goldstein DS, and Sewell L. Olfactory dysfunction in pure autonomic failure: Implications for the pathogenesis of Lewy body diseases. Parkinsonism Relat Disord. 2009;15(7):516-20.
66. Lenka A, Lamotte G, and Goldstein DS. Cardiac (18)F-dopamine PET distinguishes PD with orthostatic hypotension from Parkinsonian MSA. Mov Disord Clin Pract. 2021;8(4):582-6.
67. Tanei ZI, Saito Y, Ito S, Matsubara T, Motoda A, Yamazaki M, et al. Lewy pathology of the esophagus correlates with the progression of Lewy body disease: a Japanese cohort study of autopsy cases. Acta Neuropathol. 2021;141(1):25-37.
68. Harapan BN, Frydrychowicz C, Classen J, Wittekind C, Gradistanac T, Rumpf JJ, et al. No

enhanced (p-) alpha-synuclein deposition in gastrointestinal tissue of Parkinson's disease patients. Parkinsonism Relat Disord. 2020;80:82-8.

69. Bu LL, Huang KX, Zheng DZ, Lin DY, Chen Y, Jing XN, et al. Alpha-Synuclein Accumulation and Its Phosphorylation in the Enteric Nervous System of Patients Without Neurodegeneration: An Explorative Study. Front Aging Neurosci. 2020;12:575481.
70. Isonaka R, Rosenberg AZ, Sullivan P, Corrales A, Holmes C, Sharabi Y, et al. Alpha-Synuclein deposition within sympathetic noradrenergic neurons is associated with myocardial noradrenergic deficiency in neurogenic orthostatic hypotension. Hypertension. 2019;73(4):910-8.
71. Wolfovitz E, Grossman E, Folio CJ, Keiser HR, Kopin IJ, and Goldstein DS. Derivation of urinary dopamine from plasma dihydroxyphenylalanine in humans. Clin Sci. 1993;84:549-57.
72. Goldstein DS, Mezey E, Yamamoto T, Aneman A, Friberg P, and Eisenhofer G. Is there a third peripheral catecholaminergic system? Endogenous dopamine as an autocrine/paracrine substance derived from plasma DOPA and inactivated by conjugation. Hypertens Res. 1995;18 Suppl 1:S93-S9.
73. Eisenhofer G, Aneman A, Hooper D, Rundqvist B, and Friberg P. Mesenteric organ production, hepatic metabolism, and renal elimination of norepinephrine and its metabolites in humans. J Neurochem. 1996;66:1565-73.
74. Eisenhofer G, Aneman A, Friberg P, Hooper D, Fandriks L, Lonroth H, et al. Substantial production of dopamine in the human gastrointestinal tract. J Clin Endocrinol Metab. 1997;82(11):3864-71.
75. Jinsmaa Y, Sharabi Y, Sullivan P, Isonaka R, and Goldstein DS. 3,4-Dihydroxyphenylacetaldehyde-induced protein modifications and their mitigation by N-acetylcysteine. J Pharmacol Exp Ther. 2018;366(1):113-24.
76. Jinsmaa Y, Isonaka R, Sharabi Y, and Goldstein DS. 3,4-Dihydroxyphenylacetaldehyde is more efficient than dopamine in oligomerizing and quinonizing alpha-synuclein. J

Pharmacol Exp Ther. 2020;372(2):157-65.

77. Winner B, Jappelli R, Maji SK, Desplats PA, Boyer L, Aigner S, et al. In vivo demonstration that alpha-synuclein oligomers are toxic. Proc Natl Acad Sci USA. 2011;108(10):4194-9.
78. Wilson EO. Consilience: The Unity of Knowledge. New York, NY: Vintage Books; 1998.
79. Eisenhofer G, Pacak K, Goldstein DS, Chen C, and Shulkin B. 123I-MIBG scintigraphy of catecholamine systems: impediments to applications in clinical medicine. Eur J Nucl Med. 2000;27(5):611-2.
80. Lamotte G, and Goldstein DS. What new can we learn from cardiac sympathetic neuroimaging in synucleinopathies? Clin Auton Res. 2022;32(2):95-8.
81. Doty RL, Deems DA, and Stellar S. Olfactory dysfunction in parkinsonism: a general deficit unrelated to neurologic signs, disease stage, or disease duration. Neurology. 1988;38(8):1237-44.
82. Boeve BF, Silber MH, and Ferman TJ. REM sleep behavior disorder in Parkinson's disease and dementia with Lewy bodies. J Geriatr Psychiatry Neurol. 2004;17(3):146-57.
83. Gomperts SN. Lewy Body Dementias: Dementia With Lewy Bodies and Parkinson Disease Dementia. Continuum. 2016;22(2 Dementia):435-63.
84. McKeith IG, Boeve BF, Dickson DW, Halliday G, Taylor JP, Weintraub D, et al. Diagnosis and management of dementia with Lewy bodies: Fourth consensus report of the DLB Consortium. Neurology. 2017;89(1):88-100.
85. Goldstein DS, Eldadah BA, Holmes C, Pechnik S, Moak J, Saleem A, et al. Neurocirculatory abnormalities in Parkinson disease with orthostatic hypotension: independence from levodopa treatment. Hypertension. 2005;46(6):1333-9.
86. Goldstein DS. Dysautonomia in Parkinson's disease: neurocardiological abnormalities. Lancet Neurol. 2003;2(11):669-76.
87. Littell RC, Milliken GA, Stroup WW, and Wolfinger RD. Cary, NC: SAS Institute; 1996.
88. Huang Q. PharmaSUG. China; 2015.

89. Rahman F, and Goldstein DS. Quantitative indices of baroreflex-sympathoneural function. Clin Auton Res. 2014;24:103-10.

FIGURES AND FIGURE LEGENDS

Figure 1: Participants in the PDRisk study

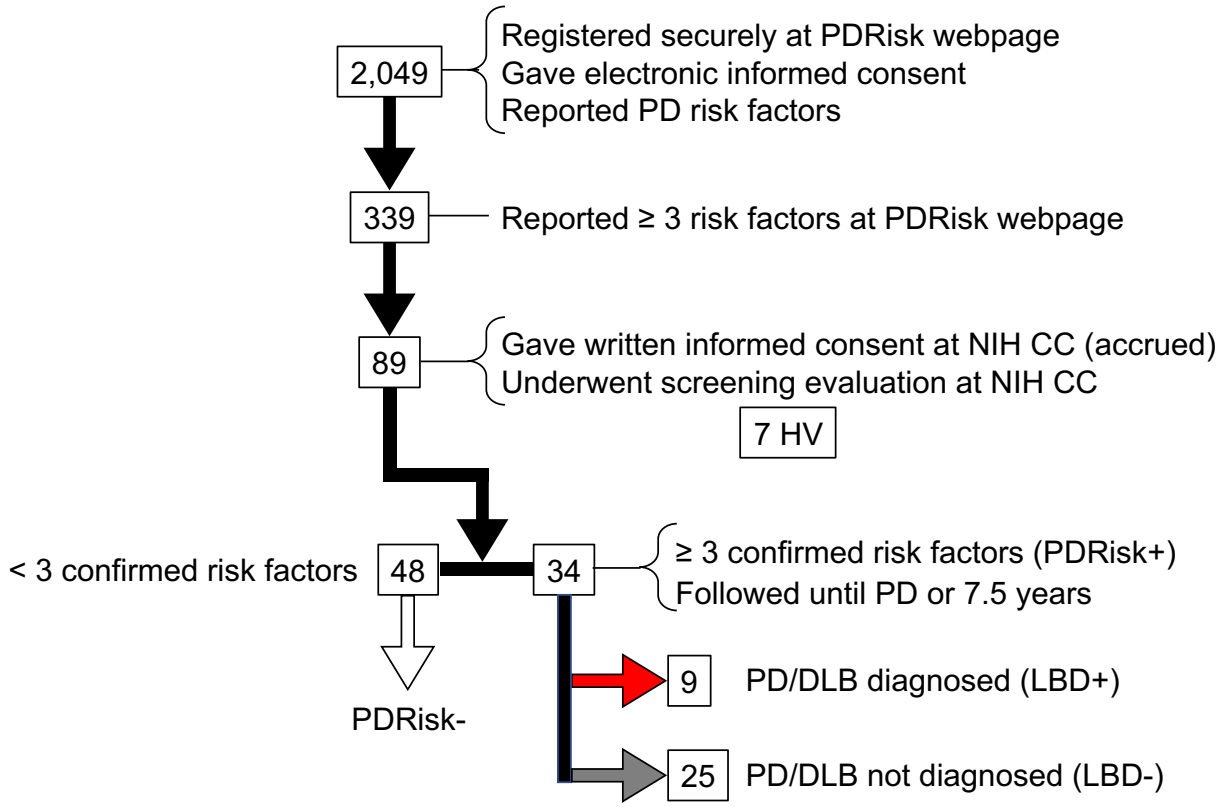
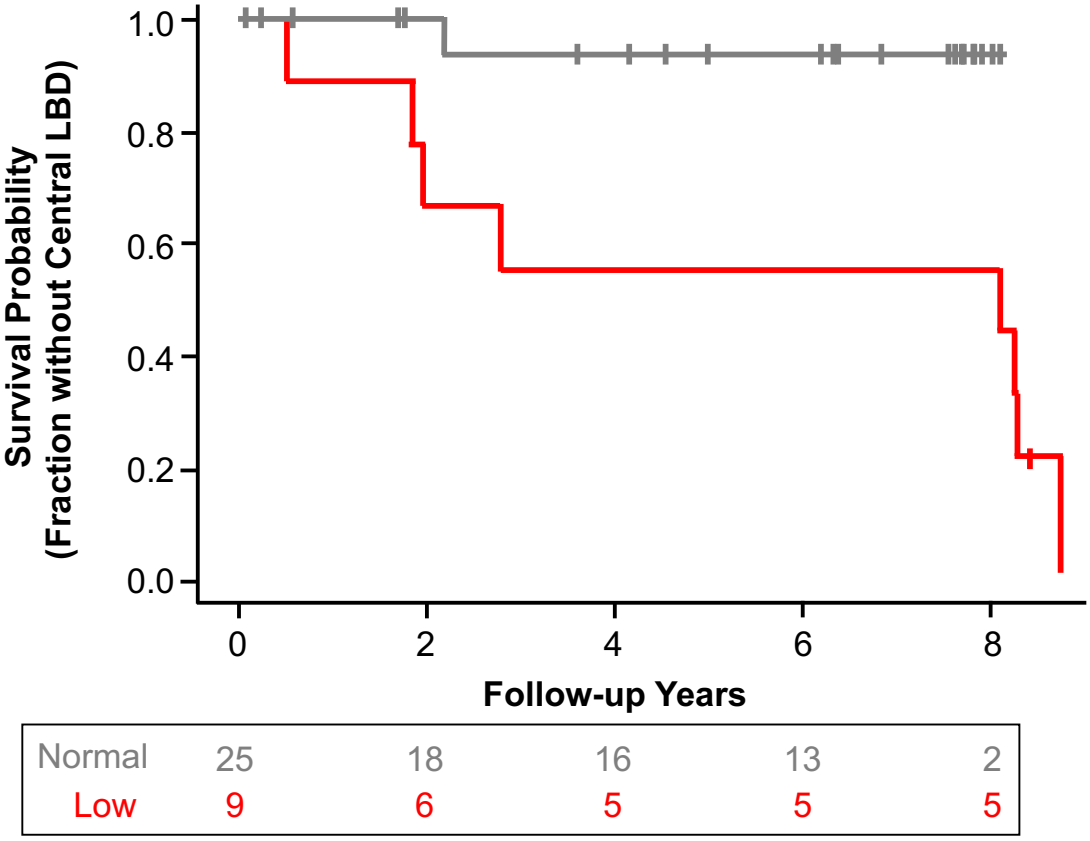
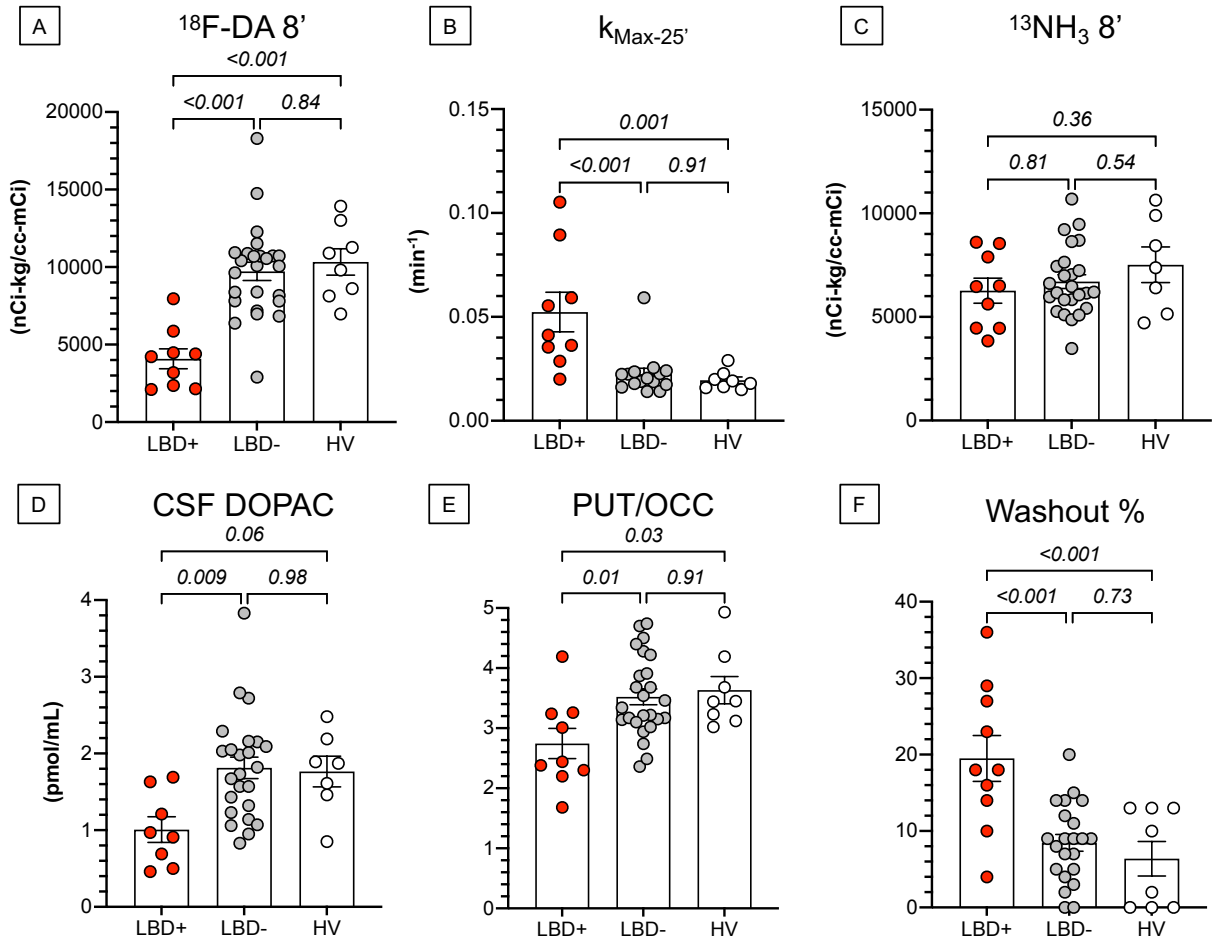


Figure 2: Survival probability (fraction without a central Lewy body disease (LBD)) as a function of years of follow-up in at-risk individuals stratified in terms of the initial interventricular septum [18]F-dopamine ([18]F-DA)-derived radioactivity.



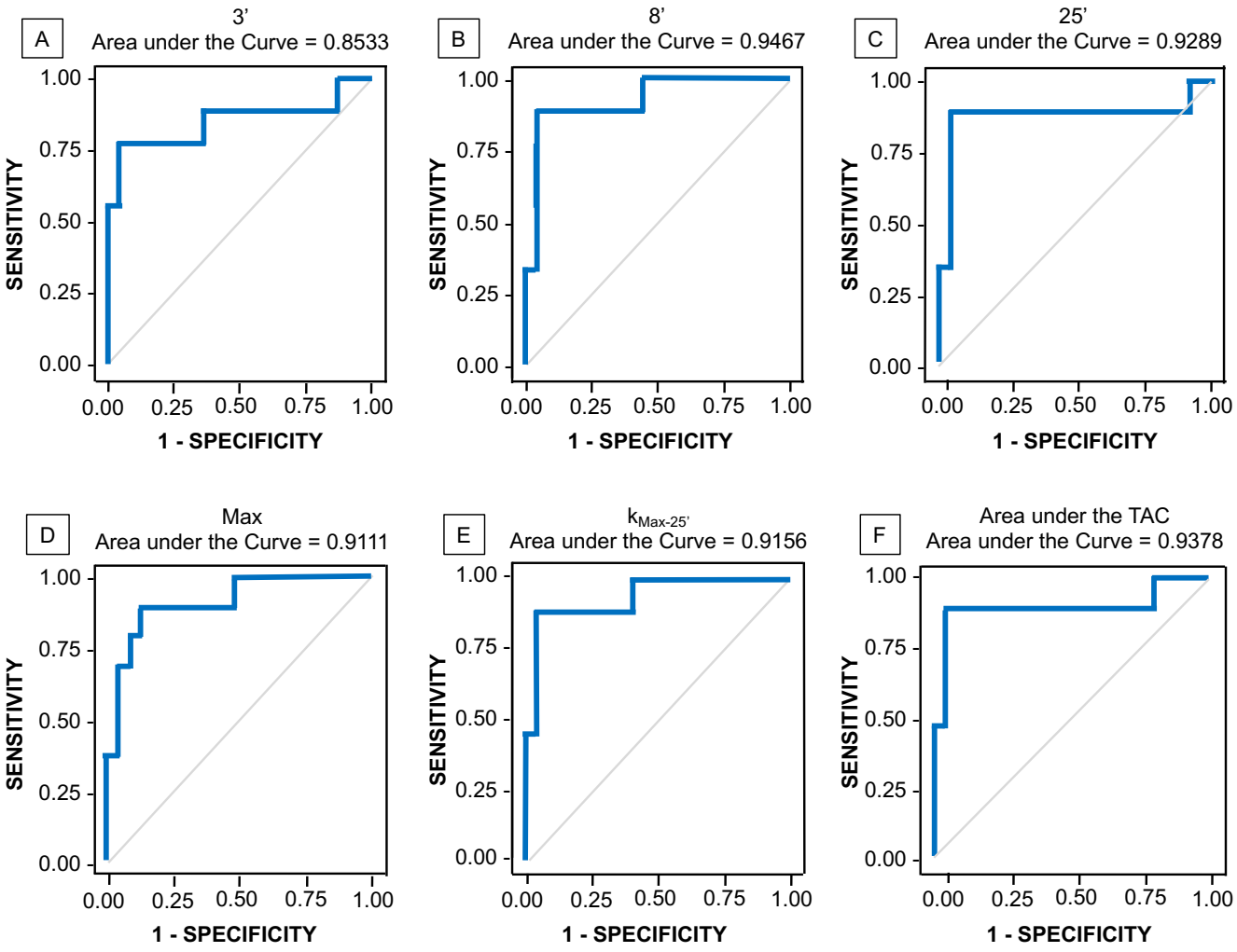
The difference in survival time (without LBD) between low and normal [18]F-DA-derived radioactivity was significant with p=0.0091 by Log-rank test. The bottom two lines represent the numbers of subjects remaining at risk with normal (>6,000 nCi-kg/cc-mCi) or low (<6,000 nCi-kg/cc-mCi) radioactivity.

Figure 3: Individual and mean (± SEM) values for cardiac positron emission tomographic data and biomarkers of central dopaminergic innervation in at-risk individuals who subsequently were diagnosed with a central Lewy body disease (LBD+) or were not diagnosed with a central Lewy body disease (LBD-) and concurrently studied healthy volunteers (HV).



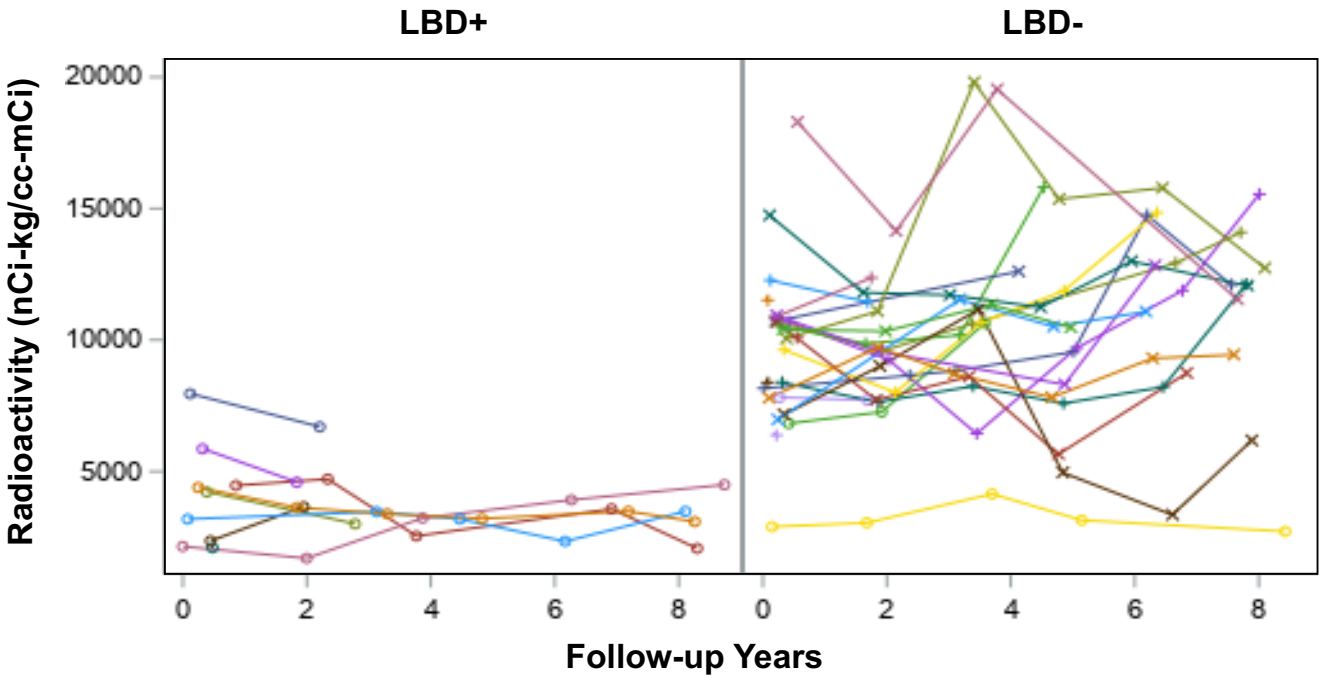
(A) [18]F-Dopamine ([18]F-DA)-derived radioactivity in the dynamic PET frame with midpoint 8' after initiation of intravenous administration of the tracer. (B) Mono-exponential slope of decline in [18]F-dopamine-derived radioactivity across the time points from the maximum value to the value in the dynamic frame with midpoint 25' after initiation of infusion of the tracer. (C) [13]N-Ammonia- ($^{13}NH_3$)-derived radioactivity in the dynamic PET frame with midpoint 8' after initiation of intravenous administration of the tracer. (D) Cerebrospinal fluid concentration of 3,4-dihydroxyphenylacetic acid. (E) Putamen/occipital (PUT/OCC) cortex ratios of [18]F-DOPA-derived radioactivity. (F) Percent decrease in putamen [18]F-DOPA-derived radioactivity between the 15' static scan beginning 30' after intravenous administration of the tracer and the 15' static scan ending 120' after administration of the tracer.

Figure 4: Receiver operating characteristic curves for interventricular septal myocardial [18]F-dopamine-derived radioactivity (9 LBD+ 25 LBD-).



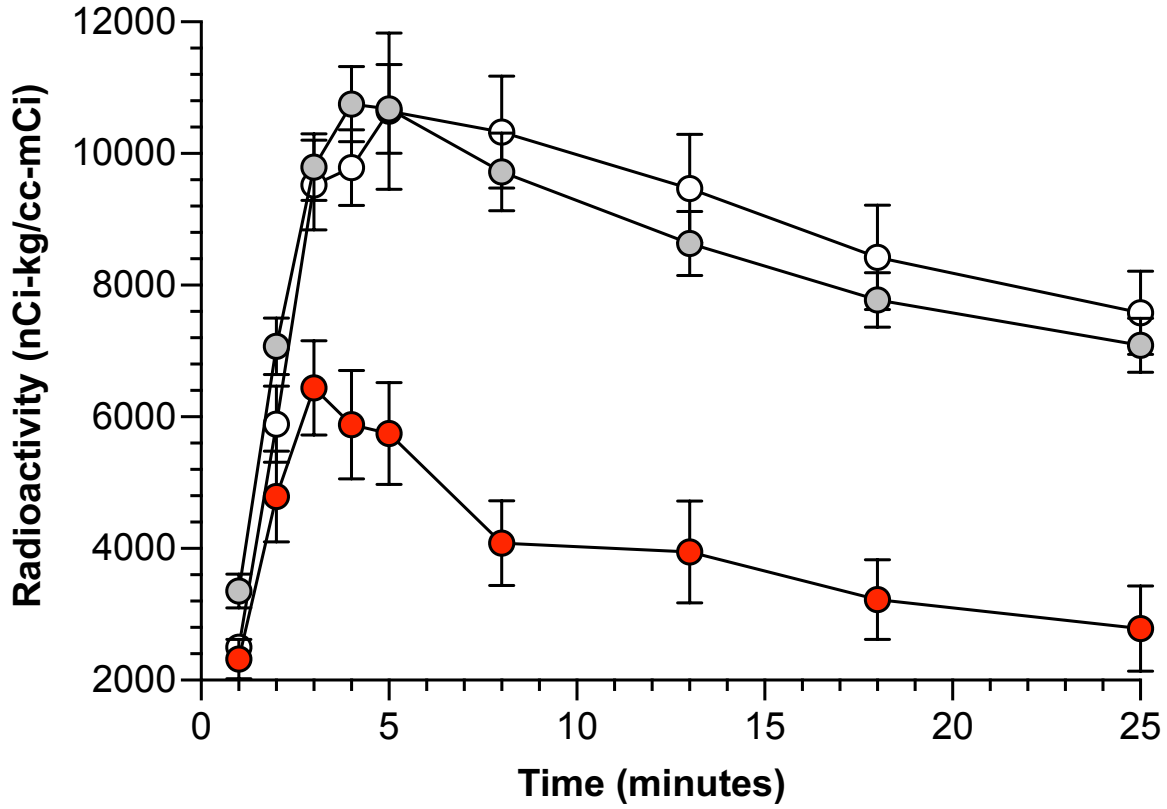
(A) [18]F-Dopamine ([18]F-DA)-derived radioactivity in the dynamic PET frame with midpoint 3' after initiation of intravenous administration of the tracer. (B) [18]F-DA-derived radioactivity in the dynamic PET frame with midpoint 8' after initiation of intravenous administration of the tracer. (C) [18]F-DA-derived radioactivity in the dynamic PET frame with midpoint 25' after initiation of intravenous administration of the tracer. (D) Maximum [18]F-DA-derived radioactivity among the dynamic PET frames. (E) Mono-exponential slope of decline in [18]F-dopamine-derived radioactivity across the time points from the maximum value to the value in the dynamic frame with midpoint 25' after initiation of infusion of the tracer. (F) Area under the curve for [18]F-DA-derived radioactivity across the dynamic PET frames.

Figure 5: Individual observed values for interventricular septal myocardial [18]F-dopamine-derived radioactivity over of years of follow-up in at-risk individuals who subsequently were diagnosed with a central Lewy body disease (LBD+, left) or were not diagnosed with a central Lewy body disease (LBD-, right) during follow-up.



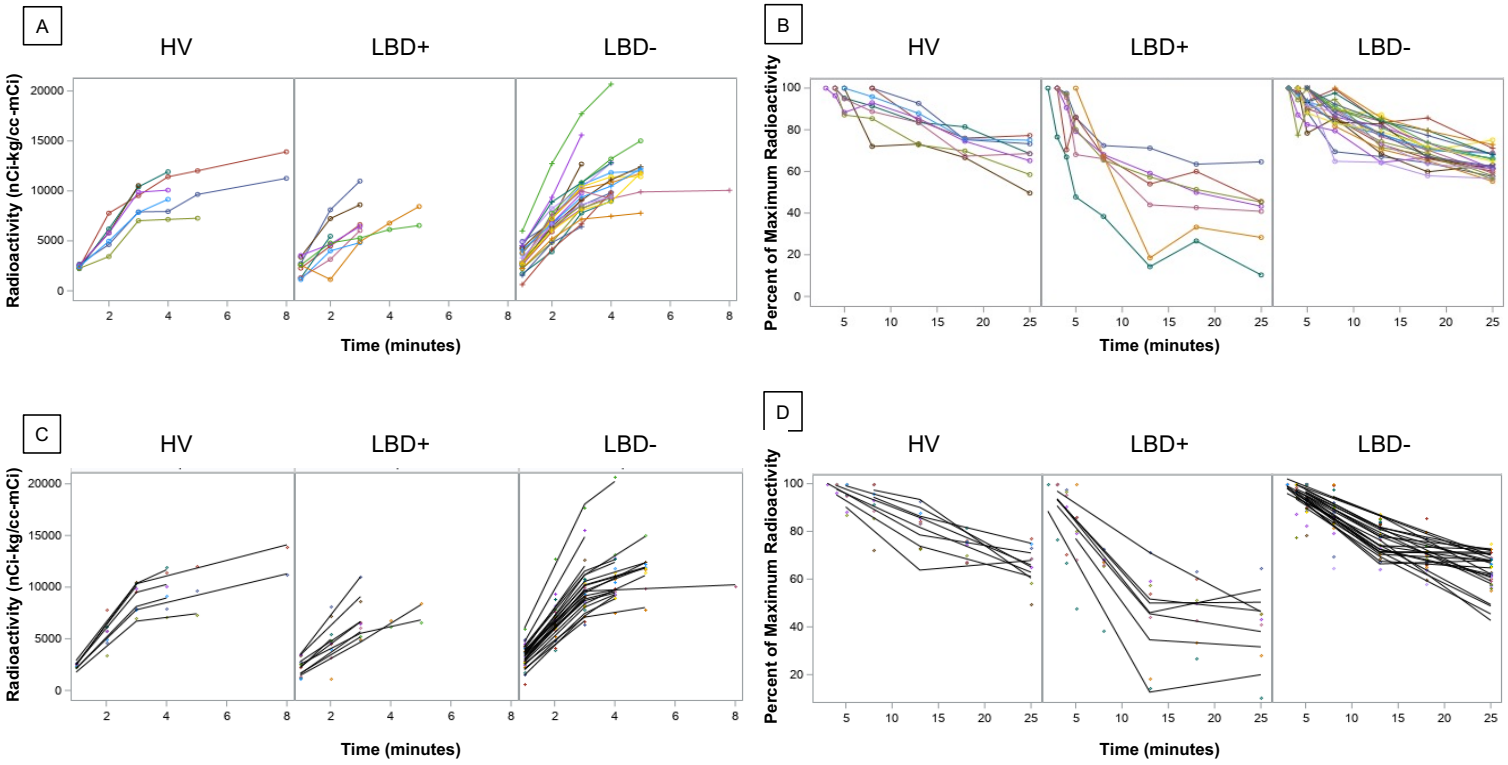
Each colored line shows data for 1 subject. (Left) Individual values for [18]F-dopamine-derived radioactivity in the 8' dynamic frame in the LBD+ group. (Right) Individual values for [18]F-dopamine-derived radioactivity in the 8' dynamic frame in the LBD- group.

Figure 6: Mean (± SEM) values for interventricular septal myocardial [18]F-dopamine-derived radioactivity in at-risk individuals who subsequently were diagnosed with a central Lewy body disease (LBD+, red, n=9) or were not diagnosed with a central Lewy body disease (LBD-, gray, n=25) and in concurrently studied healthy volunteers (HV, white, n=8).



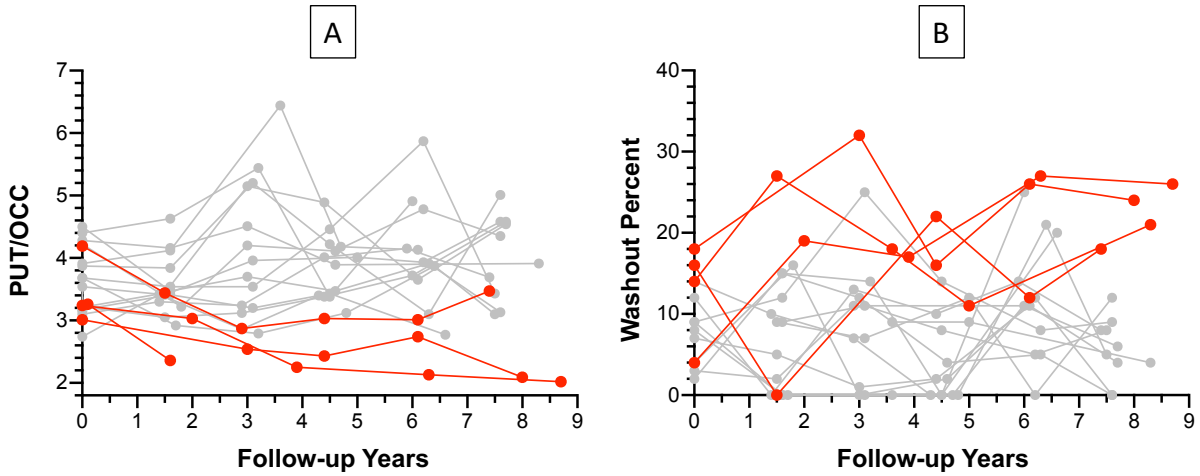
The LBD+ group has lower mean [18]F-dopamine-derived radioactivity than the LBD- and HV groups at all time points after 3' infusion of the tracer.

Figure 7: Individual observed values (A & B) and predicted curves of best fit (C & D) for interventricular septal myocardial [18]F-dopamine-derived radioactivity as a function of time from initiation of 3' intravenous administration of the tracer in healthy volunteers (HV) and in at-risk individuals who subsequently were diagnosed with a central Lewy body disease (LBD+) or were not diagnosed with a central Lewy body disease during follow-up (LBD-).



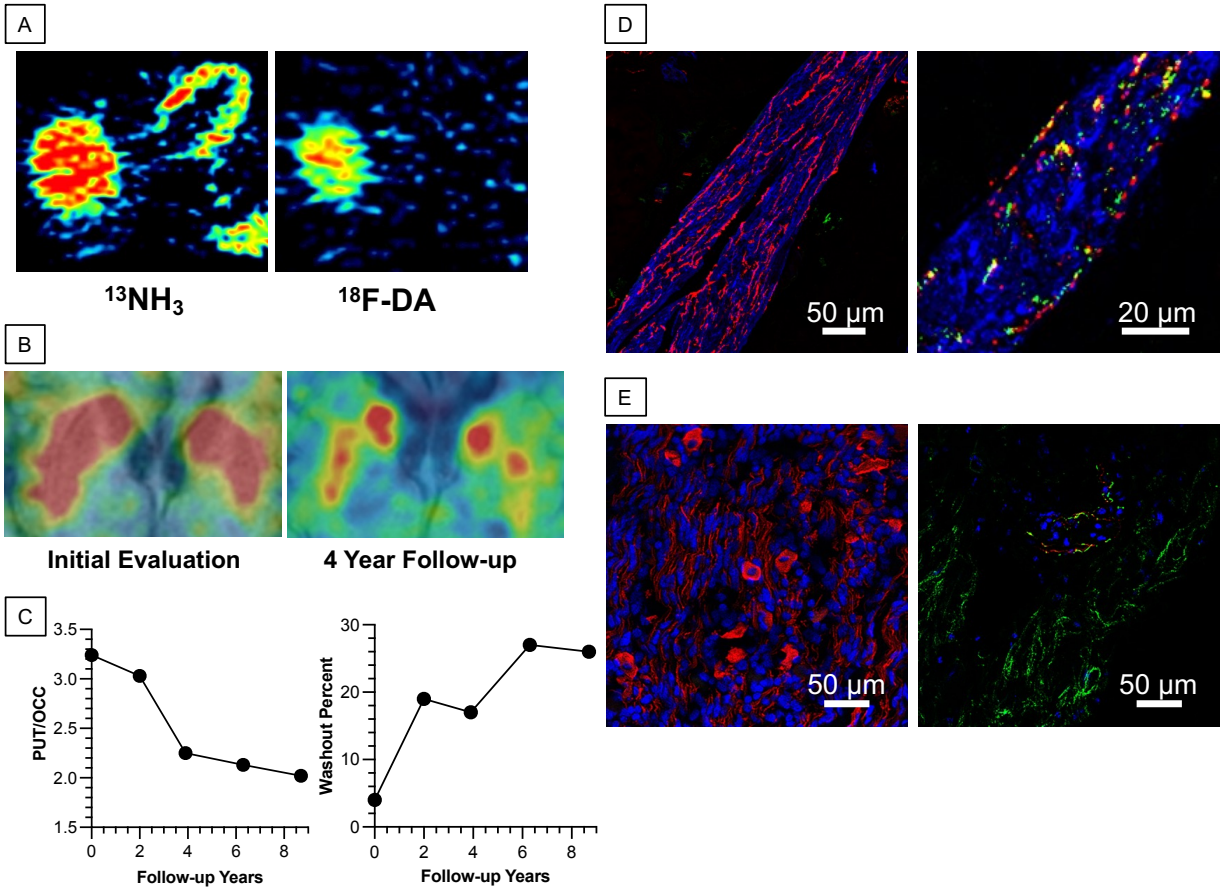
(A and C) Data from 1' after initiation of 3' intravenous administration of the tracer to the maximum radioactivity; (B and D) data from maximum radioactivity to 25' after initiation of administration of the tracer, expressed as percent of maximum radioactivity. In (A) and (C) the early increase in radioactivity is slower in the LBD+ than LBD- and HV groups. In (B) and (D) the LBD+ group has more rapid loss of radioactivity than the LBD- and HV groups between the maximum radioactivity and 13' and slower loss of radioactivity between 13' and 25'.

Figure 8: Putamen/occipital cortex ratios (PUT/OCC) (A) and washout percents of putamen [18]F-DOPA-derived radioactivity (B) in subjects developing a central Lewy body disease during follow-up (LBD+, red) and in subject not developing a central LBD after at least 4 years of follow-up (LBD-).



Data in (A) are for LBD+ participants who initially had normal PUT/OCC ratios (>2.7) and in (B) LBD+ participants who initially had normal washout percents (<20%). PUT/OCC ratios decreased and washout percents increased between the time of the initial evaluation at the time of diagnosis with a central LBD. There was no trend over follow-up years for either variable in the LBD- subjects.

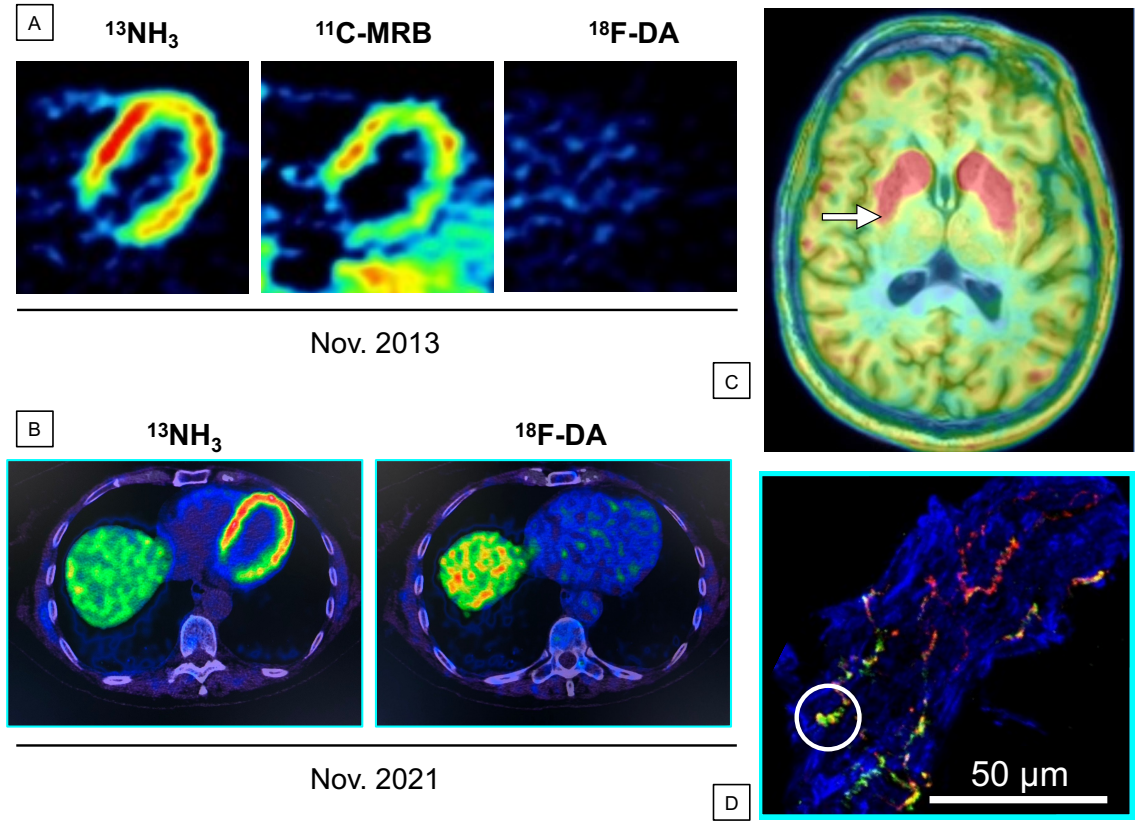
Figure 9: Positron emission tomographic (PET) data and in vivo and post-mortem immunofluorescence microscopic images from a PDRisk study participant who developed dementia with Lewy bodies and pre-terminal PD.



(A) Trans-axial PET images in the 5' dynamic frame ending about 10' after initiation of intravenous administration of 5 mCi of ^{13}N-ammonia (13NH3) and 1 mCi of ^{18}F-dopamine (^{18}F-DA). Spectral scale from minimum radioactivity in black to maximum radioactivity in red. The heart is not visible in the ^{18}F-DA image. (B) Blowup of striatal PET images (static 15' emission scans ending 120' after initiation of ^{18}F-DOPA administration) superimposed on the magnetic resonance images. Spectral scale from minimum radioactivity in black to maximum radioactivity in red. At initial evaluation the striata have normal ^{18}F-DOPA-derived radioactivity; at 4 years of follow-up there is bilaterally decreased putamen (PUT) radioactivity. (C) (left) PUT/occipital cortex (PUT/OCC) ratios (average of the 2 sides) of ^{18}F-DOPA-derived radioactivity (15'

emission scans ending 120' after initiation of [18]F-DOPA administration) as a function of years of follow-up. The normal cutoff value is 2.7. During follow-up the patient's PUT/OCC ratio declined in a tri-phasic manner, with a steep decrease between 2 and 4 years and slower subsequent decreases. (right) washout percents of PUT [1]8F-DOPA-derived radioactivity from the 15' emission scan beginning 30' after initiation of tracer administration to the 15' scan ending 120' after initiation of tracer administration. The normal cutoff is 20%. During follow-up the washout percents increase to persistently increased values. (D) Immunofluorescence confocal microscopic images of arrector pili muscles in skin biopsies from a control subject (left) and the patient (right). Blue=smooth muscle actin, red=tyrosine hydroxylase (TH), green=alpha-synuclein (α-syn), yellow=α-syn-TH colocalization. There are abundant TH-positive fibers and no visible α-syn in the control arrector pili muscle. There is α-syn-TH colocalization in the patient (colocalization index 1.6, upper limit of normal=1.5).(70) (E) Post-mortem sympathetic ganglion tissue from a control subject (left) and the patient (right). Blue=DAPI (cell nuclei), red=tyrosine hydroxylase (TH), green=alpha-synuclein (α-syn), yellow=α-syn-TH colocalization. There are abundant TH-positive neurons and fibers and no visible α-syn in the control subject. There is a loss of cellularity with severely decreased TH and an abundance of α-syn fibrils in the patient.

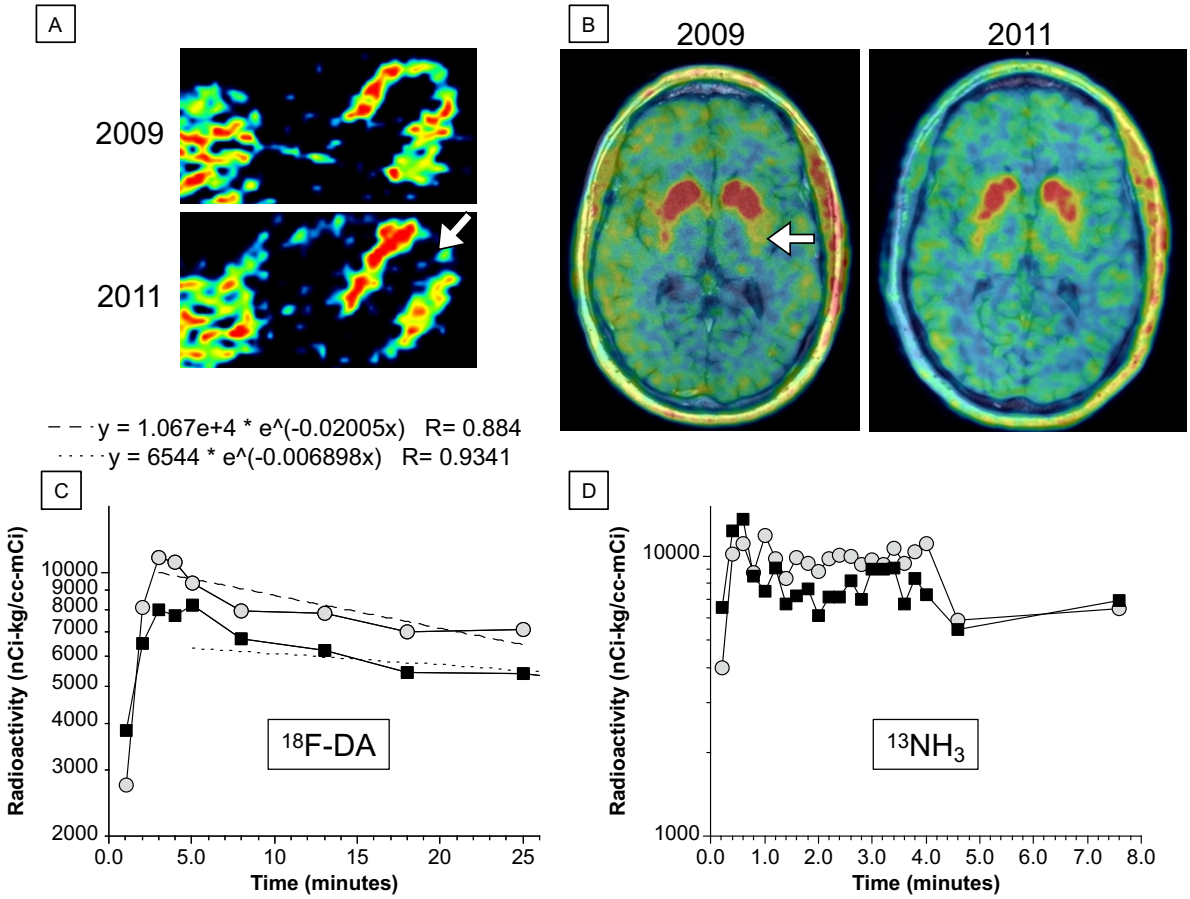
Figure 10: Positron emission tomographic (PET) and immunofluorescence microscopic images from a PDRisk study participant whose condition evolved from pure autonomic failure to PD with orthostatic hypotension.



(A) Trans-axial PET images of the heart (left) in the 5' dynamic frame ending about 10' after initiation of intravenous administration of 5 mCi of ^{13}N-ammonia ($^{13}NH_3$), (center) in the 15' static frame ending about 38' after initiation of intravenous administration of 10 mCi of ^{11}C-methylreboxetine (^{11}C-MRB), and (right) in the 5' dynamic frame ending about 10' after initiation of intravenous administration of 1 mCi of ^{18}F-dopamine (^{18}F-DA). Spectral scale from minimum radioactivity in black to maximum radioactivity in red. (B) Trans-axial PET images in the 5' dynamic frames ending about 10' after initiation of intravenous administration of (left) 5 mCi of ^{13N}H3 and (right) 1 mCi of ^{18}F-DA). Spectral scale from minimum radioactivity in black to maximum radioactivity in red. (C) Trans-axial PET image (static 15' emission scans ending 120' after initiation of ^{18}F-DOPA administration) superimposed on the magnetic resonance

image. Spectral scale from minimum radioactivity in black to maximum radioactivity in red. The posterior putamen has decreased [18]F-DOPA-derived radioactivity (PUT/occipital cortex (PUT/OCC) ratio on the right side = 1.88, normal cutoff value = 2.7. (D) Immunofluorescence confocal microscopic image of arrector pili muscles in a skin biopsy from the patient. Blue=smooth muscle actin, red=tyrosine hydroxylase (TH), green=alpha-synuclein (α-syn), yellow=α-syn-TH colocalization. There is increased α-syn-TH colocalization (white circle), with an α-syn-TH colocalization index of 2.1 (upper limit of normal=1.5) (70).

Figure 11: PET imaging in a PDRisk study participant upon initial evaluation and 2.2 years later, when PD was diagnosed.



(A) Lower thoracic transaxial [18]F-dopamine images for the 5' dynamic frame with midpoint 8' after initiation of tracer administration. The maximum radioactivity is in red and minimum black on a spectral scale for each image. Arrow indicates decreased apical and inferolateral wall radioactivity in 2011 compared to the same regions in 2009. (B) Transaxial [18]F-DOPA/MRI scans for the 15' static emission scan ending 120' after tracer administration. Between 2009 and 2011 there is progressive loss of putamen [18]F-DOPA-derived radioactivity. Arrow indicates decreased radioactivity in the posterior putamen. (C) Interventricular septal myocardial [18]F-dopamine-derived radioactivity as a function of time during and after 3'-intravenous infusion of the tracer. Upon initial evaluation (gray circles) the time-activity curve and the slope of mono-exponential decline from the peak radioactivity were normal. At 2.2 years of follow-up the

participant, newly diagnosed with PD, had decreased but still normal peak radioactivity and a normal slope of decline in radioactivity. (D) Myocardial perfusion indicated by ^{13}N-ammonia-derived radioactivity was about the same for the initial evaluation and 1.6 years of follow-up.

Table 1: ANCOVAs for interventricular septal ^{18}F-dopamine-derived radioactivity in the PDRisk study (with development of a central Lewy body disease (LBD+, N=9), without development of a central Lewy body disease (LBD-, N=25), and Healthy Volunteers (HV, N=8)).

Biomarker	Least Squares Mean			Group F	p
	LBD+	LBD-	HV	(df=2)	
^{18}F-DA 3'	6113	9923	9482	21.13	<0.0001
^{18}F-DA 8'	3581	9918	10268	22.42	<0.0001
^{18}F-DA 25'	2502	7198	7549	8.91	0.0007
^{18}F-DA Max	6530	11664	11459	12.37	<0.0001
$k_{Max-25'}$	0.0513	0.0223	0.0194	15.1	<0.0001
Area TAC	3421	8315	8494	21.12	<0.0001

Data are shown for the least squares means adjusted for age for interventricular septal ^{18}F-dopamine- (^{18}F-DA)-derived radioactivity in the 3' dynamic frame (midpoint about 3 minutes after initiation of infusion), the 8' frame (midpoint about 8' minutes after initiation of infusion), the 25' frame (midpoint about 25 minutes after initiation of infusion), maximum (Max) radioactivity, the slope of the mono-exponential decline in radioactivity from the maximum radioactivity to 25' (k_{Max-25}), and the area under the time-radioactivity curve (TAC) for the entire time series. Tukey's method was used for multiple comparisons among groups. For all 6 outcome variables the difference between the LBD+ and the LBD- and HV groups was significant ($p<0.01$). The HV and LBD- groups did not differ significantly ($p>0.5$).

Table 2: Receiver operating characteristic curve analyses for the separability of the LBD+ and LBD- groups. Results are tabulated for all 9 subjects in the LBD+ group, the entire LBD- group regardless of the duration of follow-up (N=25) and the LBD- subgroup with at least 7 years of follow-up (N=11).

N=34 (LBD+ and Entire LBD- group)

Biomarker	AUC	Chi-square	p-value	Threshold	Sensitivity	Specificity
^{18}F-DA 3’	0.8533	12.2	0.0005	≤ 6633	78	96
^{18}F-DA 8’	0.9467	125.5	<0.0001	≤ 5867	89	96
^{18}F-DA 25’	0.9289	63.3	<0.0001	≤ 3730	89	96
^{18}F-DA Max	0.9111	49.2	<0.0001	≤ 8613	89	88
^{18}F-DA $k_{Max-25'}$	0.9156	36.7	<0.0001	≥ 0.0287	89	96
^{18}F-DA Area TAC	0.9378	81.0	<0.0001	≤ 5073	89	96

N=20 (LBD+ group and 11 LBD- participants with ≥ 7 years follow-up)

Biomarker	AUC	Chi-square	p-value	Threshold	Sensitivity	Specificity
^{18}F-DA 3’	0.8788	15.9	<0.0001	≤ 6633	78	100
^{18}F-DA 8’	0.9192	39.9	<0.0001	≤ 5867	89	91
^{18}F-DA 25’	0.899	28.2	<0.0001	≤ 3730	89	91
^{18}F-DA Max	0.9293	44.6	<0.0001	≤ 8613	89	91
^{18}F-DA $k_{Max-25'}$	0.8889	22.3	<0.0001	≥ 0.0287	89	91
^{18}F-DA Area TAC	0.9091	35.4	<0.0001	≤ 5073	89	91

Abbreviations: AUC=area under the ROC curve. See Legend for Table 1 for other definitions.

Table 3: Piecewise linear random coefficient model analysis for interventricular septal myocardial [18]F-dopamine-derived radioactivity in two different time intervals: for time from 1' to peak time and for time=peak time to 25'.

Part I: Time from 1' to Peak Time (breakpoint at time=3')

	Estimate	Standard Error	t Value	Pr > |t|
Slope estimate: Time=1' to 3'				
HV	3321.13	348.74	9.52	<0.0001
LBD+	2261.83	317.66	7.12	<0.0001
LBD-	3274.34	189.68	17.26	<0.0001
Slope estimate: Time=3' to Peak				
HV	825.46	344.74	2.39	0.0294
LBD+	1537.03	580.58	2.65	0.0153
LBD-	1174.08	211.44	5.55	<0.0001
Slope comparison: Time =1' to 3'				
HV vs. LBD+			2.25	0.0309
HV vs. LBD-			0.12	0.9069
LBD- vs. LBD+			2.74	0.0094
Slope comparison: Time =3' to Peak				
HV vs. LBD+			-1.05	0.3052
HV vs. LBD-			-0.86	0.4002
LBD- vs. LBD+			0.59	0.5633
Slope comparison: Time ≤3' vs. ≥3'				
HV			-5.68	<0.0001
LB+			-1.15	0.2604
LBD-			-7.97	<0.0001

Part II: Time from Peak Time to 25' (Standardized by Maximum radioactivity, breakpoint at time=13')

	Estimate	Standard Error	t Value	Pr > |t|
Slope estimate: Peak Time to 13'				
HV	-1.70	0.39	-4.40	<0.0001
LBD+	-4.65	0.34	-13.76	<0.0001
LBD-	-2.28	0.21	-10.84	<0.0001
Slope estimate: Time 13' to 25'				
HV	-1.24	0.16	-7.74	<0.0001
LBD+	-0.27	0.16	-1.75	0.0867
LBD-	-1.09	0.09	-12.12	<0.0001
Slope comparison: Peak Time to 13'				
HV vs. LBD+			5.75	<0.0001
HV vs. LBD-			1.31	0.1925
LBD- vs. LBD+			5.96	<0.0001
Slope comparison: Time =13' to 25'				
HV vs. LBD+			-4.33	<0.0001
HV vs. LBD-			-0.82	0.4188
LBD- vs. LBD+			4.55	<0.0001
Slope comparison: Time <13' vs. ≥13'				
HV			0.90	0.3681
LBD+			9.67	<0.0001
LBD-			4.27	<0.0001

Time ≤3' is for the time interval from the initiation of tracer administration until the 3' frame; Peak is for the frame with maximum radioactivity. **Part I**: one subject (LBD- #21) with outliers was excluded from the analysis. For Time ≤3', radioactivity increased in all three groups. The

slope of increase was smaller in the LBD+ than in LBD- and HV groups. Between 3' and Peak radioactivity the radioactivity increased further; the groups did not differ in slope in this time interval. In all 3 groups the slope for Time ≤3' was greater than for Time ≥3'. **Part II:** In all 3 groups radioactivity decreased between the time of Peak radioactivity and 13'. In this interval there was more rapid loss of radioactivity in the LBD+ than in the LBD- and HV groups. Between 13' and 25' the decrease in radioactivity was slower in the LBD+ than in the LBD- and HV groups.

Supplementary Table 1: Individual demographic, clinical, physiological, neurochemical, and neuroimaging data from the PDRisk study (PDRisk+, PDRisk-, HV; N=86).

Clinical Tab Abbreviations:

Betablk.=beta-adrenoceptor blocker; CNCS=Clinical Neurocardiology Section database; COMTI=catechol-O-methyltransferase inhibitor; CQ10=coenzyme Q10; DA Agonist=dopamine receptor agonist; FH/Occup.=family history/occupation; Florinef=fludrocortisone; HV=healthy volunteers; LBD-=Lewy body disease not diagnosed during follow-up; LBD+=Lewy body disease diagnosed during follow-up; MoCA=Montreal Cognitive Assessment; MRI=magnetic resonance imaging; MVI=multivitamin; N/A=not applicable; Orth.=orthostatic; PDRisk-=less than 3 confirmed risk factors; PPI=proton pump inhibitor; Rx=medication; SSRI=selective serotonin reuptake inhibitor; UPDRS=Unified Parkinson Disease Rating Scale; UPSIT=University of Pennsylvania Smell Identification Test

Neurochemical Tabs Abbreviations:

Δ=change from baseline; BL=baseline; CSF=cerebrospinal fluid; DA=dopamine; DHPG=3,4-dihydroxyphenylglycol; DOPA=3,4-dihydroxyphenylalanine; DOPAC=3,4-dihydroxyphenylacetic acid; EPI=epinephrine; FxΔ=fractional from from baseline; LP=lumbar puncture; NE=norepinephrine; Ortho=orthostasis (head-up tilt). Red-highlighted cells indicate statistically significant differences between the LBD+ and LBD- groups by independent-means t-tests.

Physiological Tab Abbreviations:

ΔBPd=change in diastolic blood pressure from supine rest to head-up tilt; ΔBPs=change in systolic blood pressure from supine rest to head-up tilt; ΔHR=change in heart rate from supine rest to head-up tilt; ΔMAP=change in mean arterial blood pressure from supine rest to head-up tilt; Baro. Area II=baroreflex area Phase II; Baro. Area III-IV=baroreflex area in Phases III-IV; Baro. Area Total=baroreflex area sum of Phase II+Phase III-IV; BPd=diastolic blood pressure; BPs=systolic blood pressure; CVNN=coefficient of variation of the cardiac interbeat interval; Fall in BPs Val=fall in systolic blood pressure from Phase I to the nadir pressure in Phase II of

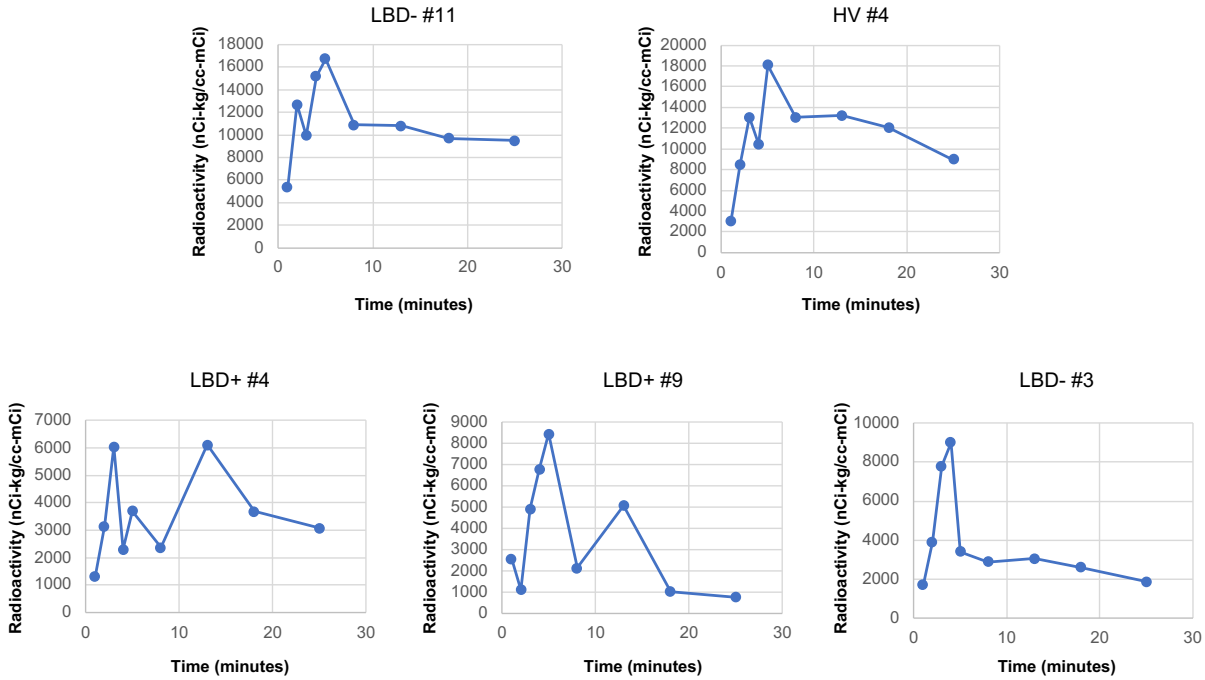
the Valsalva maneuver; HF=high frequency power; Inc. in HR Val=increase in heart rate from Phase I to the nadir blood pressure in Phase II of the Valsalva maneuver; LF Power=low frequency power; LF/HF=LF power/HF power; MAP=mean arterial pressure; NN=cardiac interbeat interval; NU=normalized power; PRT=pressure recovery time; SDNN=standard deviation of the cardiac interbeat interval; SV Supine=cardiac stroke volume during supine rest; TP=total power; Val=Valsalva maneuver

Neuroimaging Tab Abbreviations:

03N0004=NIH Clinical Protocol 03N0004; 13NH3=^{13}N-ammonia; 18F-DA=^{18}F=dopamine; ANT=anterior; CAU:SN=caudate/substantia nigra ratio; CAU/PUT=head of the caudate/putamen ratio; CAUD/OCC=head of the caudate/occipital cortex ratio; CAUD=head of the caudate; CBL=cerebellum; Chamb.=left ventricular chamber; Eval.=evaluation; GP/PUT=globus pallidus/putamen ratio; GP=globus pallidus; k(Max to 25')=$k_{Max\text{-}25'}$; L=left; Max=maximum radioactivity; NH3=^{13}N-ammonia; OCC=occipital cortex; P/A=posterior/anterior ratio in the putamen; PET=positron emission tomography; POST=posterior; PUT:SN=putamen/substantia nigra ratio; PUT/OCC=putamen/occipital cortex ratio; PUT=putamen; R=right; SEPT or Sept.=interventricular septal myocardium; Static 1=15' static frame beginning 30' after initiation of ^{18}F-DOPA administration; SUB NIG/OCC=substantia nigra/occipital cortex ratio; SUB NIG=substantia nigra; Washout=percent decrease in putamen ^{18}F-DOPA-derived radioactivity between the first (30' from initiation of tracer administration) and second (15' frame ending 120' from initiation of tracer administration) static images

Supplementary Table 2: Pearson and Spearman correlation coefficients for correlations among biomarkers of cardiac noradrenergic and central dopaminergic deficiency in the PDRisk cohort (LBD+, LBD-, HV; N=42).

Supplementary Figure 1: Individual [18]F-dopamine-derived radioactivity vs. time curves for outliers that were not included in the breakpoint analyses.



For the analysis in Part 1, data were excluded for LBD- #11 and HV #4, because the curve did not fit the model. For the analysis in Part 2, data were excluded for LBD+ #4 and #9 and LBD- #3, for the same reason.

Supplementary Statistical Analysis Methods

The piecewise linear random coefficient model

Since [18]F-dopamine-derived radioactivity was not linear (increasing to peak and then decreasing from peak to midpoint 25'), the approximate low-rank smoother was applied to capture the trends over time using SAS procedure GLIMMIX. The Akaike information criterion (AIC) was used to determine the optimal number and location of breakpoints (interior knots) by changing the bucket size of the k-d tree. Three breakpoints at time=3, 5, 13 were constructed from the vertices of a kd-tree with the smallest AIC and best matched the expected with the observed radioactivity, in other words, a piecewise linear model with three breakpoints, which represents four linear lines with different slopes, fitted the radioactivity over the 25 minutes. However, the piecewise linear model with three breakpoints could not estimate the slopes for the second segment (time =3' to 5'). The main reason was that there were too few time points in the segment. Therefore, the radioactivity data were split into two parts: Part I included the data from 1' to the peak time (subject-based), and Part II included data from the peak time to 25'. Then, a piecewise linear random coefficient model with one breakpoint (at time=3' and 13') was applied to Part I and Part II data separately. In addition, some subjects with outliers were excluded based on the studentized residual analysis, their curve of the radioactivity within the initial PET also showed abnormal, for example, two subjects had two peaks.

In the piecewise (with one breakpoint) linear random coefficient model,

$$y = \beta_0 + \beta_1 t + \beta_2 \text{I(t -k)t} + \beta_3 \text{ group} + \beta_4 \text{ group} * \text{t} + \beta_5 \text{ group} * \text{I(t-k)} + \varepsilon$$

where y denotes the observed radioactivity

ε is the unobserved random errors

k is the breakpoint (k=3 for Part I data, k=13 for Part 2 data)

t is the time (t=1' to peak time for Part I, and t=peak time to 25 for part II data).

I(t-k) =0 for $t \le k$; I(t-k) =1for t>k.

β_0 is the intercept and is treated as a random effect

β_1 is the slope for the first segment ($t \le k$), and is treated as a random effect

β_2 is the difference in slope between the first ($t \leq k$) and second segment ($t \geq k$), and is treated as a random effect

β_3 is the group (with three levels: HV, LBD+, LBD-) effect and treated as fixed.

β_4 is the interaction between the group and β_1, which tests if the three groups have equal slopes in the first segment.

β_5 is the interaction between the group and β_2, which tests if three groups have equal difference in slope between the first and second segment. The test that the three groups have equal slopes in the second segment is constructed using the "estimate" option.

NIH Publishing Agreement & Manuscript *Cover Sheet*

By signing this Cover Sheet, the Author, on behalf of NIH, agrees to the provisions set out below, which **modify and supersede,** solely with respect to NIH, any conflicting provisions that are in the Publisher's standard copyright agreement (the "Publisher's Agreement"). If a Publisher's Agreement is attached, execution of this Cover Sheet constitutes an execution of the Publisher's Agreement, subject to the provisions and conditions of this Cover Sheet.

1. **Indemnification.** No Indemnification or "hold harmless" obligation is provided by either party.
2. **Governing Law.** This agreement will be governed by the law of the court in which a claim is brought.
3. **Copyright.** Author's contribution to the Work was done as part of the Author's official duties as a NIH employee and is a Work of the United States Government. Therefore, copyright may not be established in the United States. 17U.S.C. § 105. If Publisher intends to disseminate the Work outside of the U.S., Publisher may secure copyright to the extent authorized under the domestic laws of the relevant country, subject to a paid-up, nonexclusive, irrevocable worldwide license to the United States in such copyrighted work to reproduce, prepare derivative works, distribute copies to the public and perform publicly and display publicly the work, and to permit others to do so.
4. **No Compensation.** No royalty income or other compensation may be accepted for work done as part of official duties. The author may accept for the agency a limited number of reprints or copies of the publication.
5. **NIH Representations.** NIH represents to the Publisher that the Author is the sole author of the Author's contribution to the Work and that NIH is the owner of the rights that are the subject of this agreement; that the Work is an original work and has not previously been published in any form anywhere in the world; that to the best of NIH's knowledge the Work is not a violation of any existing copyright, moral right, database right, or of any right of privacy or other intellectual property, personal, proprietary or statutory right; that where the Author is responsible for obtaining permissions or assisting the Publishers in obtaining permissions for the use of third party material, all relevant permissions and information have been secured; and that the Work contains nothing misleading, obscene, libelous or defamatory or otherwise unlawful. NIH agrees to reasonable instructions or requirements regarding submission procedures or author communications, and reasonable ethics or conflict of interest disclosure requirements unless they conflict with the provisions of this Cover Sheet.
6. **Disclaimer.** NIH and the Author expressly disclaim any obligation in Publisher's Agreement that is not consistent with the Author's official duties or the NIH mission, described at http://www.nih.gov/about/. NIH and the Author do not disclaim obligations to comply with a Publisher's conflict of interest policy so long as, and to the extent that, such policy is consistent with NIH's own conflict of interest policies.
7. **For Peer-Reviewed Papers to be Submitted to PubMed Central.** The Author is a US government employee who must comply with the NIH Public Access Policy, and the Author or NIH will deposit, or have deposited, in NIH's PubMed Central archive, an electronic version of the final, peer-reviewed manuscript upon acceptance for publication, to be made publicly available no later than 12 months after the official date of publication. The Author and NIH agree (notwithstanding Paragraph 3 above) to follow the manuscript deposition procedures (including the relevant embargo period, if any) of the publisher so long as they are consistent with the NIH Public Access Policy.
8. **Modifications.** PubMed Central may tag or modify the work consistent with its customary practices and with the meaning and integrity of the underlying work.

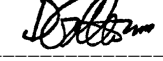
The NIH Deputy Director for Intramural Research, Michael Gottesman, M.D., approves this publishing agreement and maintains a single, signed copy of this text for all works published by NIH employees, and contractors and trainees who are working at the NIH. No additional signature from Dr. Gottesman is needed.

Author's name: David S. Goldstein

Author's Institute or Center: NINDS, NIH Check if Publisher' Agreement is attached ☐

Name of manuscript/work: **Cardiac noradrenergic deficiency revealed by ^{18}F-dopamine positron emission tomography identifies preclinical central Lewy body diseases**

Name of publication: Journal of Clinical Investigation



_____ May 18, 2023

Author's signature Date